QUANTUM COMPUTING WITH TRAPPED IONS

www.quantenbit.de

Ferdinand Schmidt-Kaler
QUANTUM, Univ. Mainz & Helmholtz Inst. Mainz

JOHANNES GUTENBERG UNIVERSITÄT MAINZ

Bundesministerium für Bildung und Forschung

iRyd

MILLENION QUANTUM

|ATIQ⟩

IQuAn

Menue

- Trapped ion qubit introduction
- Fault-tolerant parity readout
  for quantum error correction
- Scaling up trapped ion QC technology
  Hardware & Software
- Application cases for QC
- Fast entanglement generation - Rydbergs

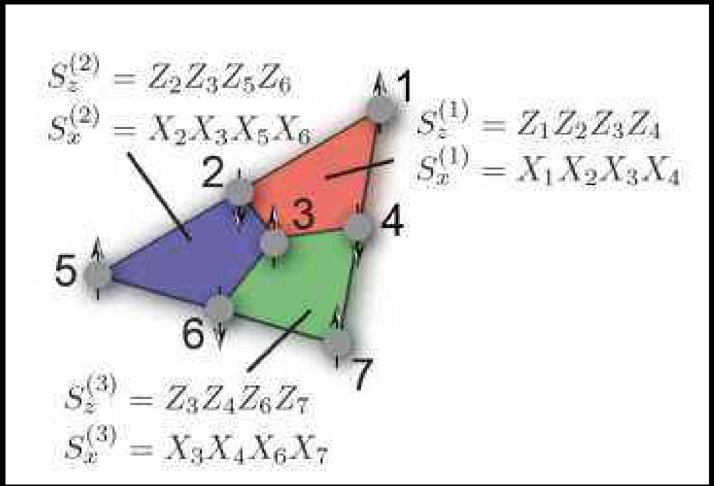

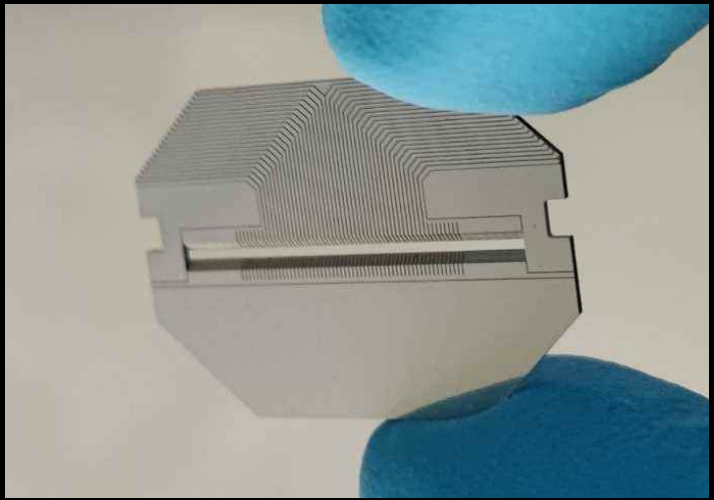

First two-qubit gate proposal

74, Number 20 4091 PHYSICAL REVIEW LETTERS 15 May 1995

Quantum Computations with Cold Trapped Ions

J. I. Cirac and P. Zoller*
Institut für Theoretische Physik, Universität Innsbruck, Technikerstrasse 25, A-6020 Innsbruck, Austria
(Received 30 November 1994)

A quantum computer can be implemented with cold ions confined in a linear trap and interacting with laser beams. Quantum gates involving any pair, triplet, or subset of ions can be realized by coupling the ions through the collective quantized motion. In this system decoherence is negligible, and the measurement (readout of the quantum register) can be carried out with a high efficiency.

Cirac, Zoller
*PRL**74**, 4091 (1995)*
*Schmidt-Kaler et al., Nat. **422**, 408 (2003)*

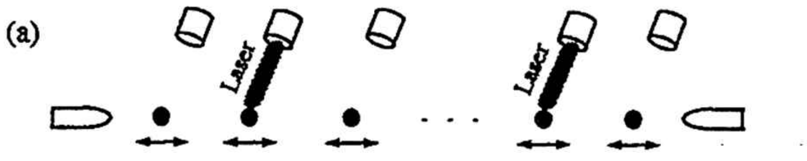

control bit

target bit

- single bit rotations and quantum gates
- small decoherence
- unity detection efficiency
- scalable …

All-to-all qubit coupling is mediated by laser light interactions and com. vibrational modes

two-qubit gate variations

- Cirac Zoller gate
- Mölmer Sörensen gate
- Spin-dependent light forces
- Spin-dependent magnetic gradient forces
- Cavity-induced interactions
- Rydberg excitation & blockade interaction
- Rydberg ultra-fast electric kick
- Atom-Ion interactions

Cirac, Zoller, PRL 74, 4091 (1995)

*Schmidt-Kaler et al., Nat. **422**, 408 (2003)*

*Sörensen, Mölmer, PRL **82**, 1971 (1999), PRA **62**, 022311 (2000)*

Leibfried et al., Nature 412, 422 (2003)

Khromova et al, PRL 108, 220502 (2012), Warring et al, Phys. Rev. A 87, 013437 (2013)

Duan, Kimble, PRL 90, 253601 (2003)

Casabone et al, PRL 111, 100505 (2013)

Takahashi, et al, PRL 124, 013602 (2020) Krutyanskiy, et al, PRL 130, 050803 (2023)

Li, Lesanowsky, Appl. Phys. B 114, 37 (2014)

Zhang, et al, Nat. 580, 345 (2020)

Vogel, et al, PRL 123, 153603 (2019)

Sencker, et al, PRA 94, 013420 (2016)

Choice of ion qubit

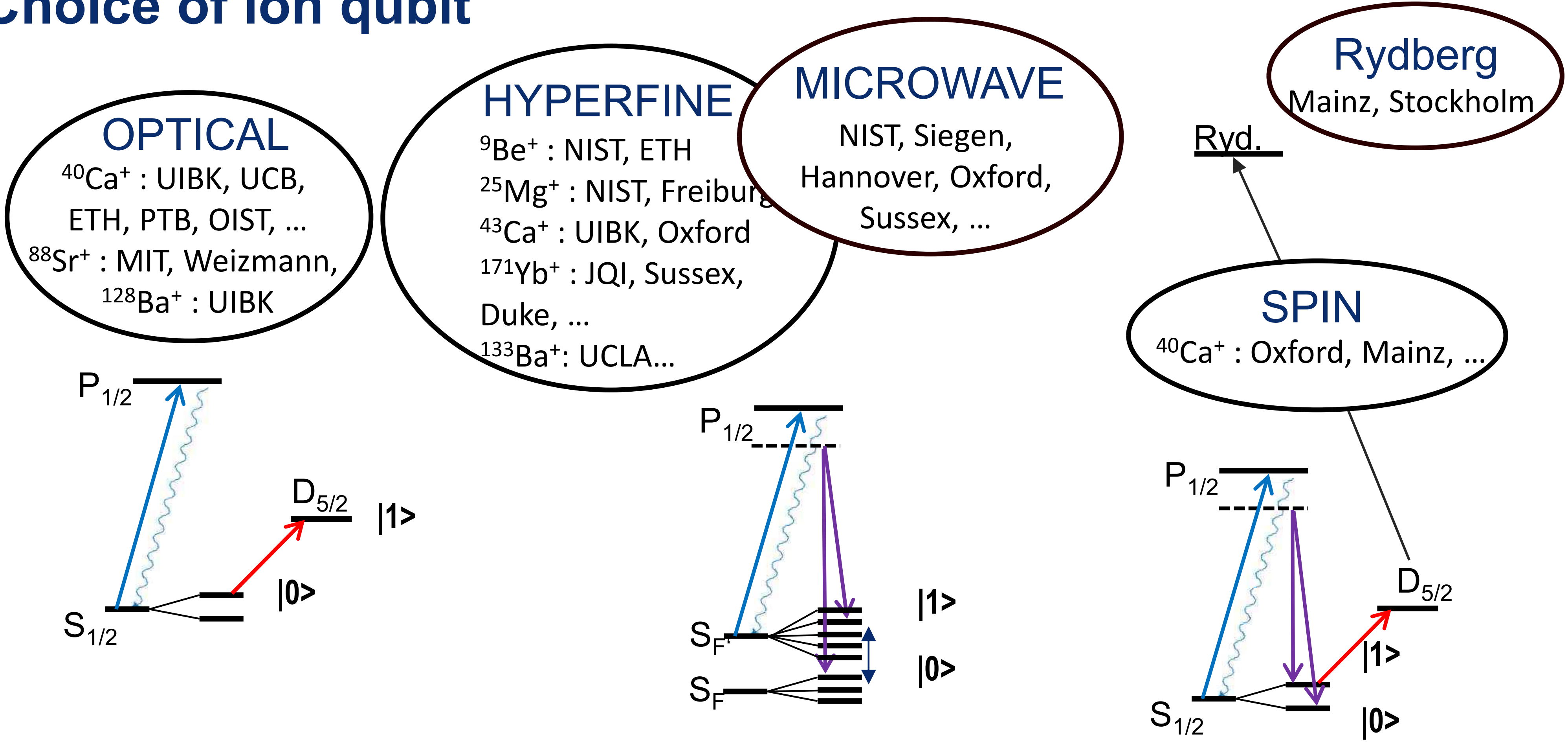

Easy readout
Requires optical phase stability
Limited by metastable lifetime

Infinite T_1
only scattering errors
complicated level scheme

Infinite T_1
only scattering errors
readout overhead

Rotation of an ion qubit

- Driven by laser beams
- >99,99% fidelity gates
- Gate time few μs

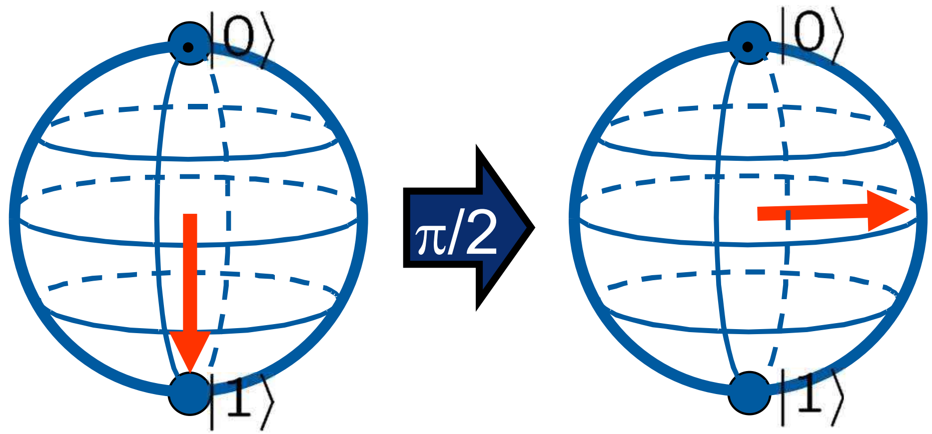

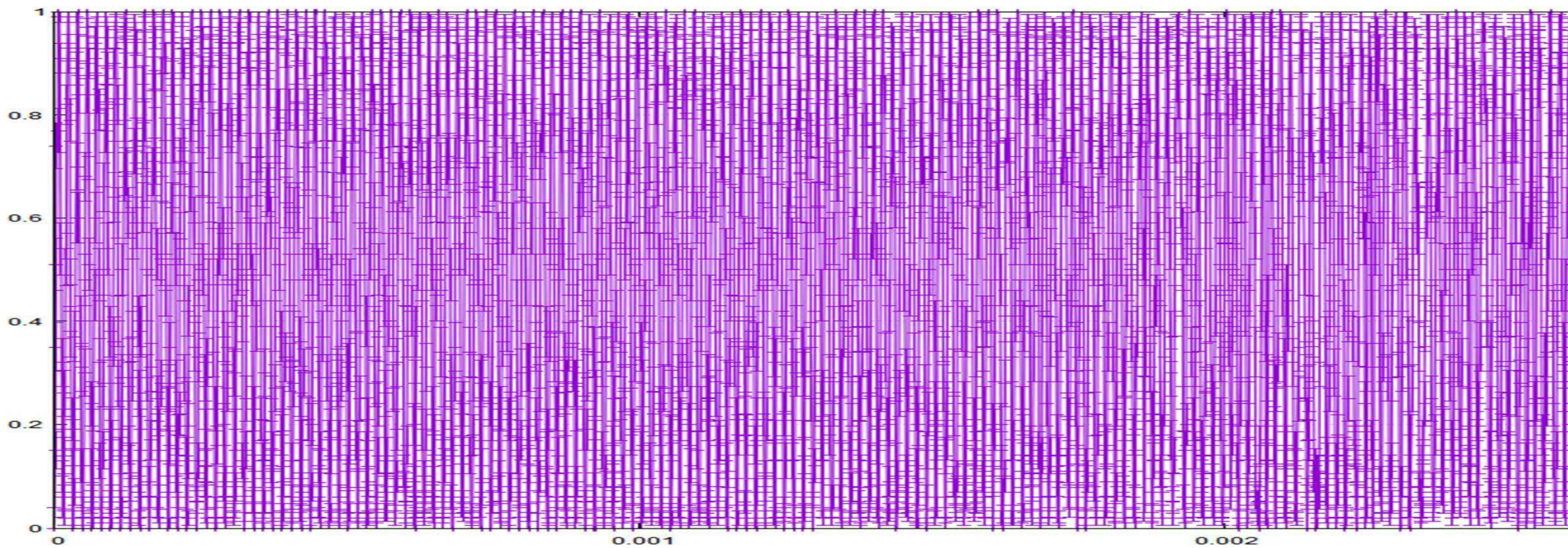

Key figures in trapped ion QC

long-range Coulomb interaction:

- ❑ All-to-all connectivity
- ❑ Single shot read-out of spin state better than $1 - 10^{-4}$
- ❑ Single gate fidelity better than $1 - 10^{-4} \ldots . 10^{-5}$
- ❑ Two qubit gate fidelity $1 – 10^{-3} \ldots . 10^{-4}$
- ❑ Two-qubit gate operation times ~ 30 … 100 µs

Quantum jumps

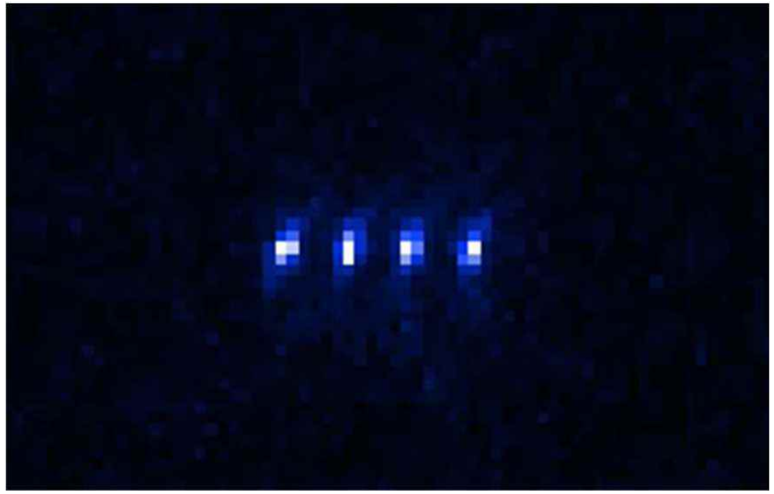

Breathing mode stroboscopic detection

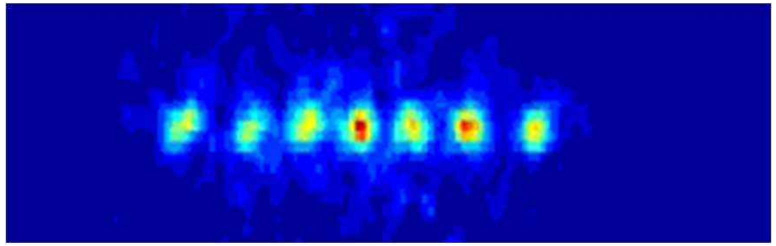

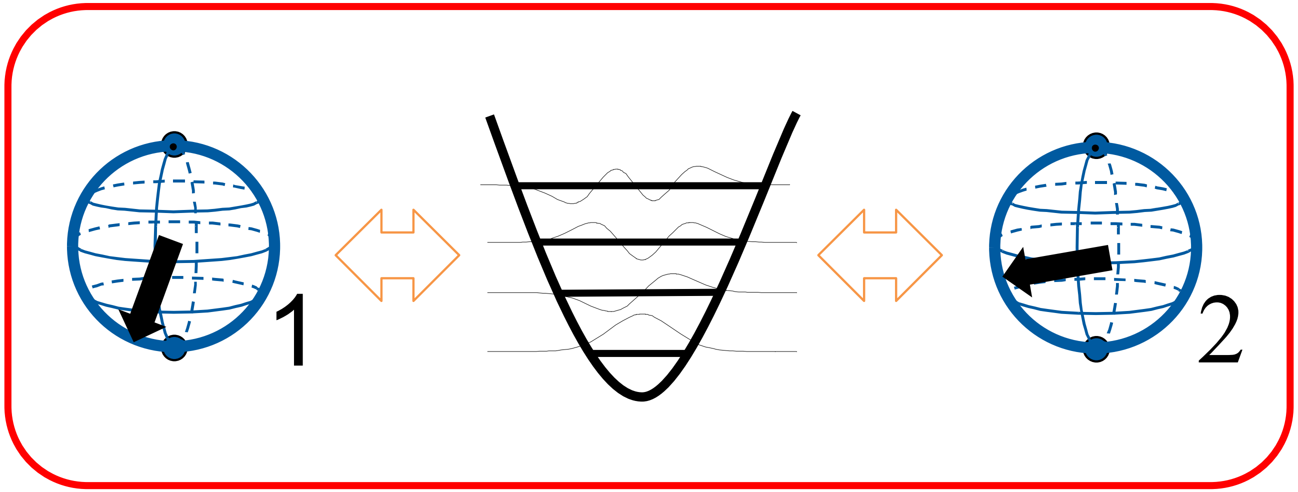

Qubit coupling is mediated by laser light interactions to one or many modes

Spin dependent light force gate

- Lin perp lin lattice generates oscillatory optical dipole force (ODF)
- Near resonant, spin-dependent excitation of gate mediating mode

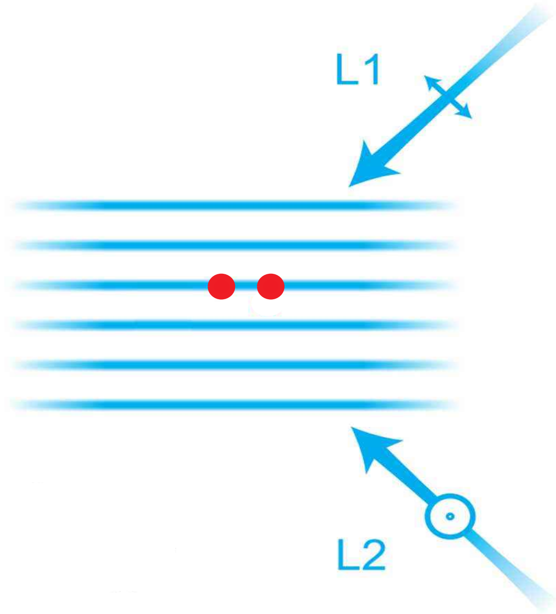

$$
\begin{aligned}
\hat{U}(t) &= \lim_{n\to\infty} \prod_{k=1}^{n} \exp\left(-\frac{\mathrm{i}}{\hbar}\hat{H}_{\mathrm{int}}(t_k)\Delta t\right) \quad \text{with } \Delta t = t/n,\ t_k = k\Delta t \\
&= \lim_{n\to\infty} \prod_{k=1}^{n} \hat{D}\left(\Omega \mathrm{e}^{\mathrm{i}\delta t_k}\Delta t\right) \\
&= \hat{D}(\alpha(t))\, \mathrm{e}^{\mathrm{i}\Phi(t)} \quad \text{with} \quad \hat{D}(\alpha(t)) = \mathrm{e}^{\alpha(t)\,\hat{a}^\dagger - \alpha^*(t)\,\hat{a}},
\end{aligned}
$$

$$\hat{H}_{\mathrm{int}}(t) = \hbar\Omega \mathrm{i}(\hat{a}^\dagger \mathrm{e}^{\mathrm{i}\delta t} - \hat{a}\mathrm{e}^{-\mathrm{i}\delta t})(\hat{\sigma}_{\mathrm{z}} \otimes \mathbb{1} + \mathbb{1} \otimes \hat{\sigma}_{\mathrm{z}})$$ for two ions and one mode

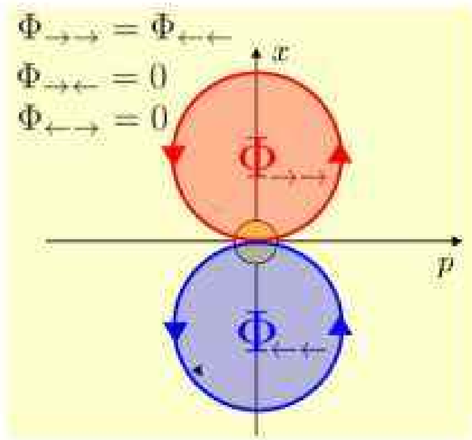

$\alpha(t) = i\frac{\Omega}{\delta}(1 - e^{i\delta t})$ displacement

$\Phi(t) = \left(\frac{\Omega}{\delta}\right)^2 (\delta t - \sin(\delta t))$ phase

δ	detuning
Ω	Amplitude
$2\pi/\delta$	return time

$$
\begin{aligned}
\{|00\rangle, |11\rangle\} &\rightarrow \mathrm{e}^{\mathrm{i}\Phi}\{|00\rangle, |11\rangle\} \\
\{|01\rangle, |10\rangle\} &\rightarrow \{|01\rangle, |10\rangle\}.
\end{aligned}
$$

Scalable quantum computing architectures

- ❑ Number of qubits
- ❑ Qubit-connectivity
- ❑ Fidelity of gate operations
- ❑ Qubit preparation & readout fidelity
- ❑ In-loop qubit readout
- ❑ Real-time feedback on quantum algorithm
- ❑ Low latency connection to high performance computer

→ Quantum-volume

→ Quantum error correction

→ Hybrid computing

Linear crystal processor

Static trapped ion registers >20 qubits

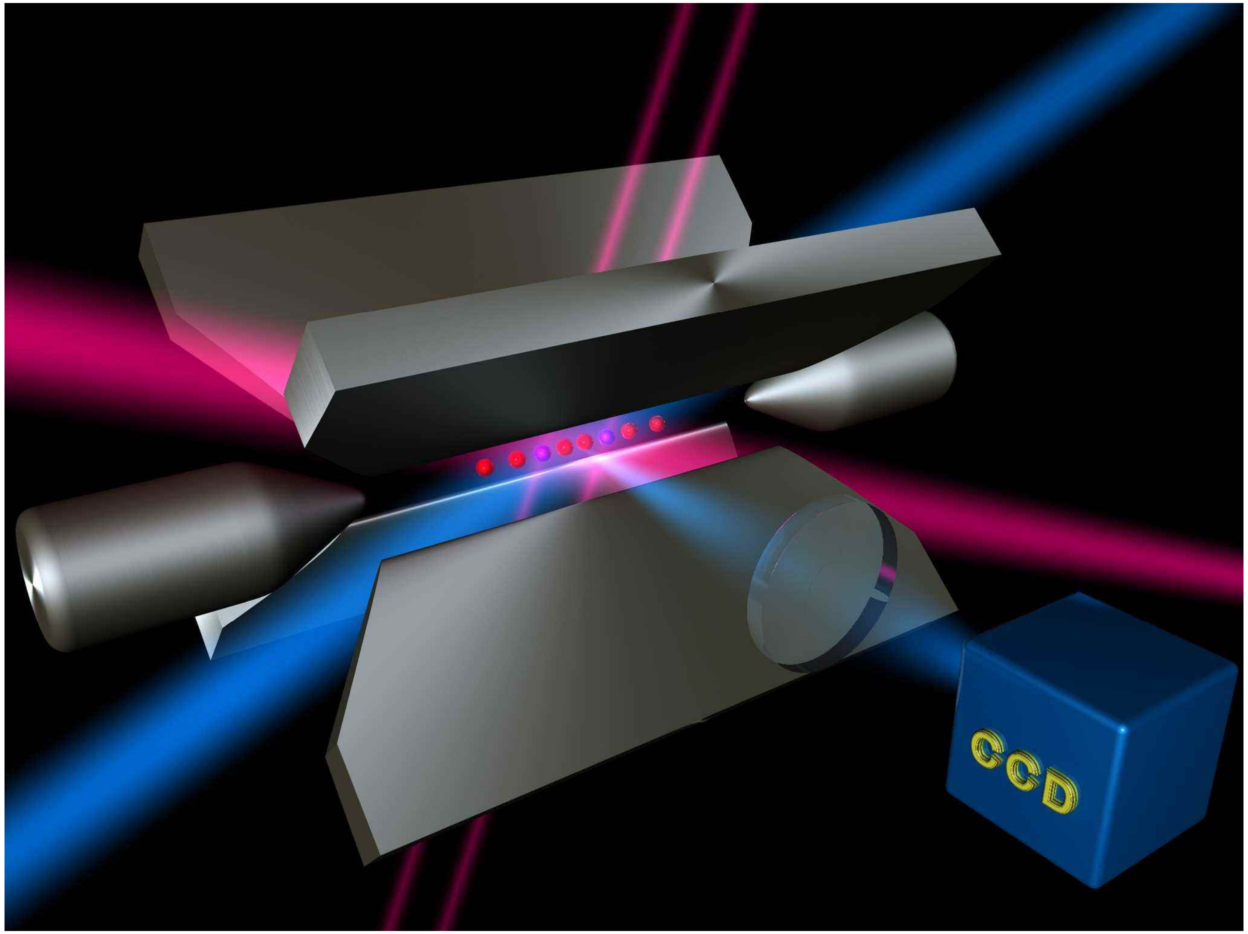

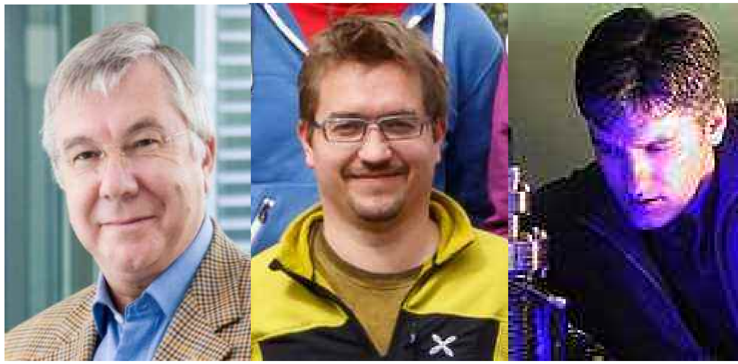

AQT IONQ

- ❑ Long linear crystals
- ❑ Individual single ion addressing for gates

Nägerl, et al, PRA 60, 145 (1999)
Friis, et al, Phys Rev X. 8 021012 (2018)
Korenblit et al, NJP 14, 095024 (2012)
Egan et al., Nat. 598, 281 (2021)

Quantum-CCD architecture

- Laser pulses generate entanglement
- Segmented micro trap allows controlling the ion positions

DIVIDE ET IMPERA

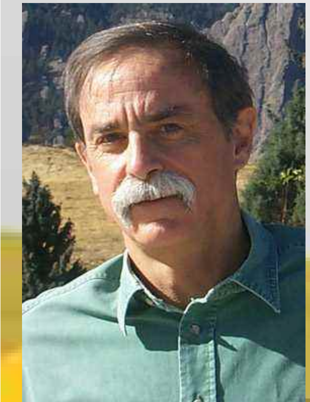

Kielpinski et al., Nat. 417, 709 (2002)

Dave Wineland – vision of scalabe QC using shuttles in segmented ion traps

Honeywell Quantum Solutions

Our quantum computing future is built on our technology heritage.

Ion movement – qubit register reconfiguration

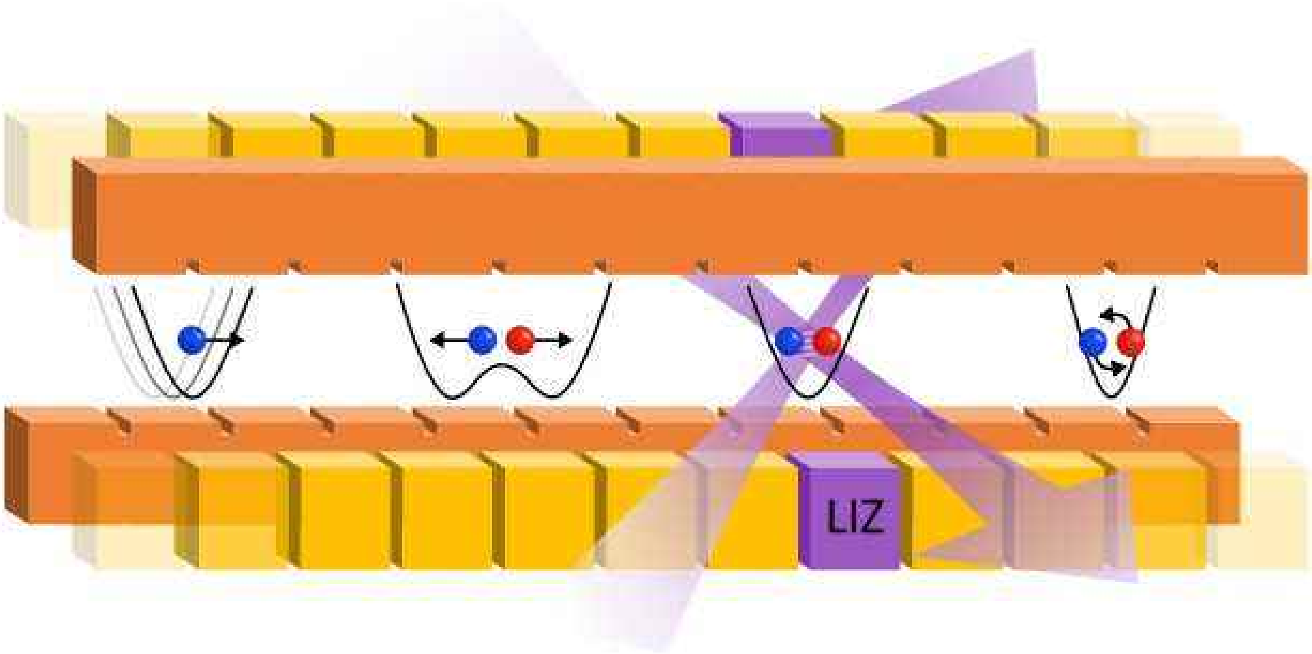

Geometric phase gate with 99.85% fidelity on **radial** mode

Single qubit rotation with average EPG of 7.8 10^{-5}

- ❑ Shuttle single ion
- ❑ Shuttle ion crystal
- ❑ Separate two-ion crystal
- ❑ Merge into two-ion crystal
- ❑ Swap ion positions

Kielpinski et al., Nat. 417, 709 (2002)
Walter et al., PRL109, 080501 (2012)
Kaufmann et al, NJP 16, 073012 (2014)
Kaufmann et al, RPA 95, 052319 (2017)
Kaufmann et al, PRL 119, 150503 (2017)
Kaustal et al, Adv. At. Mol. Opt. Phys. 69, 233 (2020)

How to digitize analog quantum errors ?

qubit $|\psi> = \alpha|0> + \beta|1>$

entangle qubit with ancilla

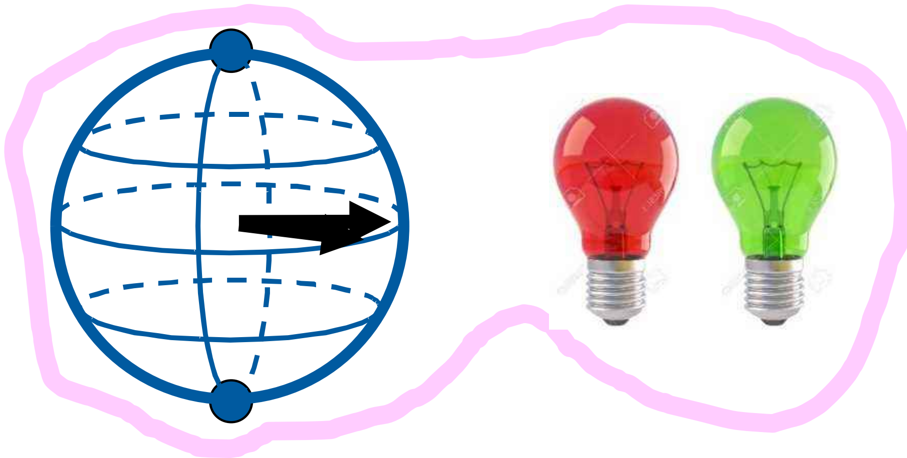

$$|\psi>_{\text{no error}} |A>_{\text{no error}} \oplus |\psi>_{\text{full error}} |A>_{\text{error}}$$

measure ancilla, and get either…

$$|\psi>_{\text{no error}} |A>_{\text{no error}} \oplus \cancel{|\psi>_{\text{full error}} |A>_{\text{error}}}$$

… or

$$\cancel{|\psi>_{\text{no error}} |A>_{\text{no error}}} \oplus |\psi>_{\text{full error}} |A>_{\text{error}}$$

Topological QEC

Bermudez et al, Phys. Rev. X 7, 041061
Nigg et al., Sci. 234, 302 (2014)

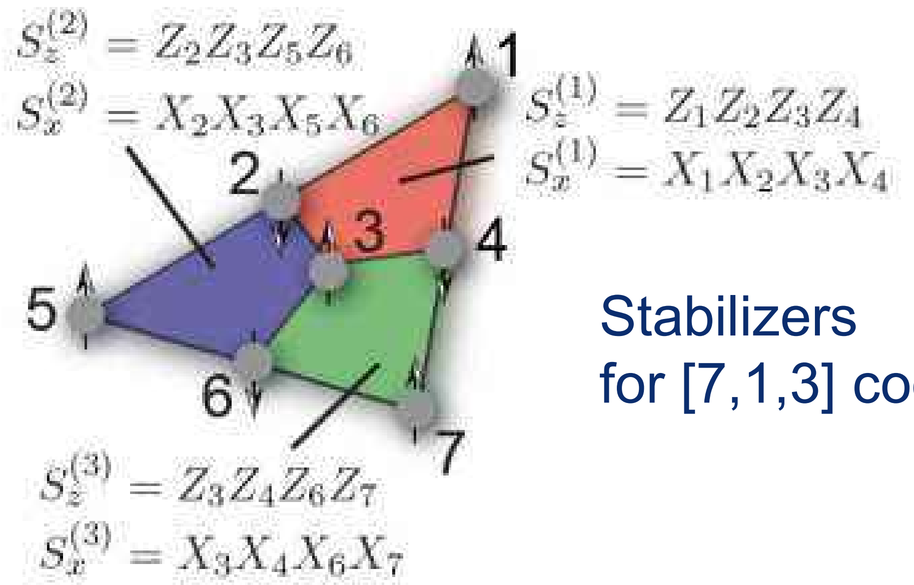

Stabilizers
for [7,1,3] code

Logical qubit using
7-data qubit color code

Bermudez et al, arXiv: 1810.09199
Chao, Reichardt, arXiv:1705.02329
Yoder, Kim, Quantum 1, 2 (2017)

Fault-tolerant syndrome readout of one plaquette

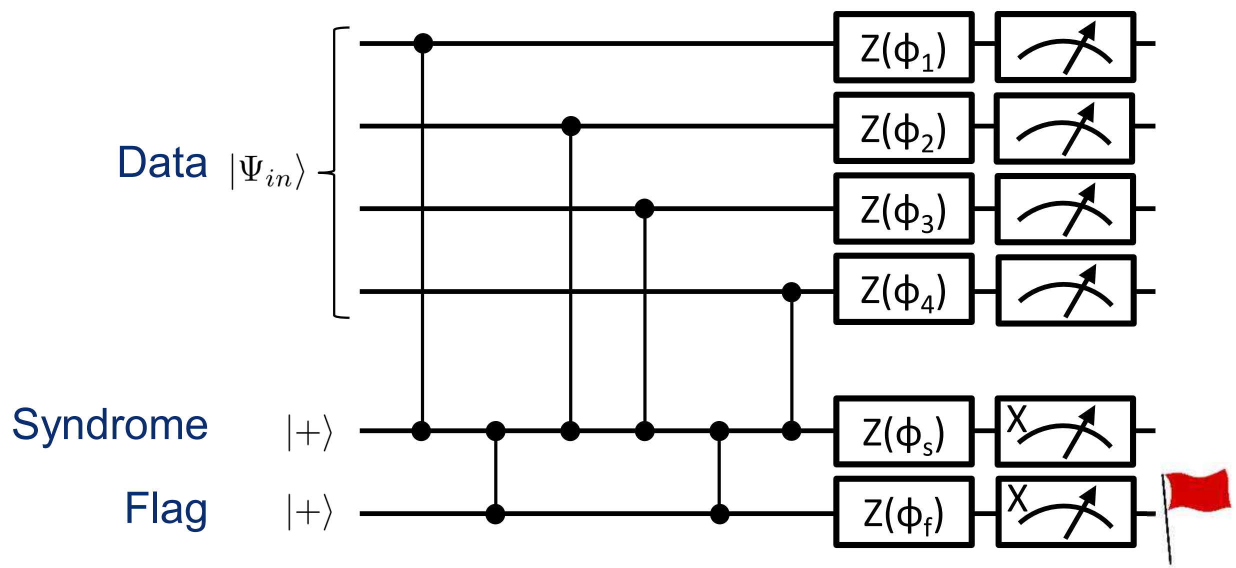

Fault-tolerant syndrome readout

6 ions:
90 configurations
41 two-ion transp.
158 single ion transp.
6 two-ion rotation
21 merge/separate
6 two-qubit gates
6 RAP pulses
6 fluo. det.

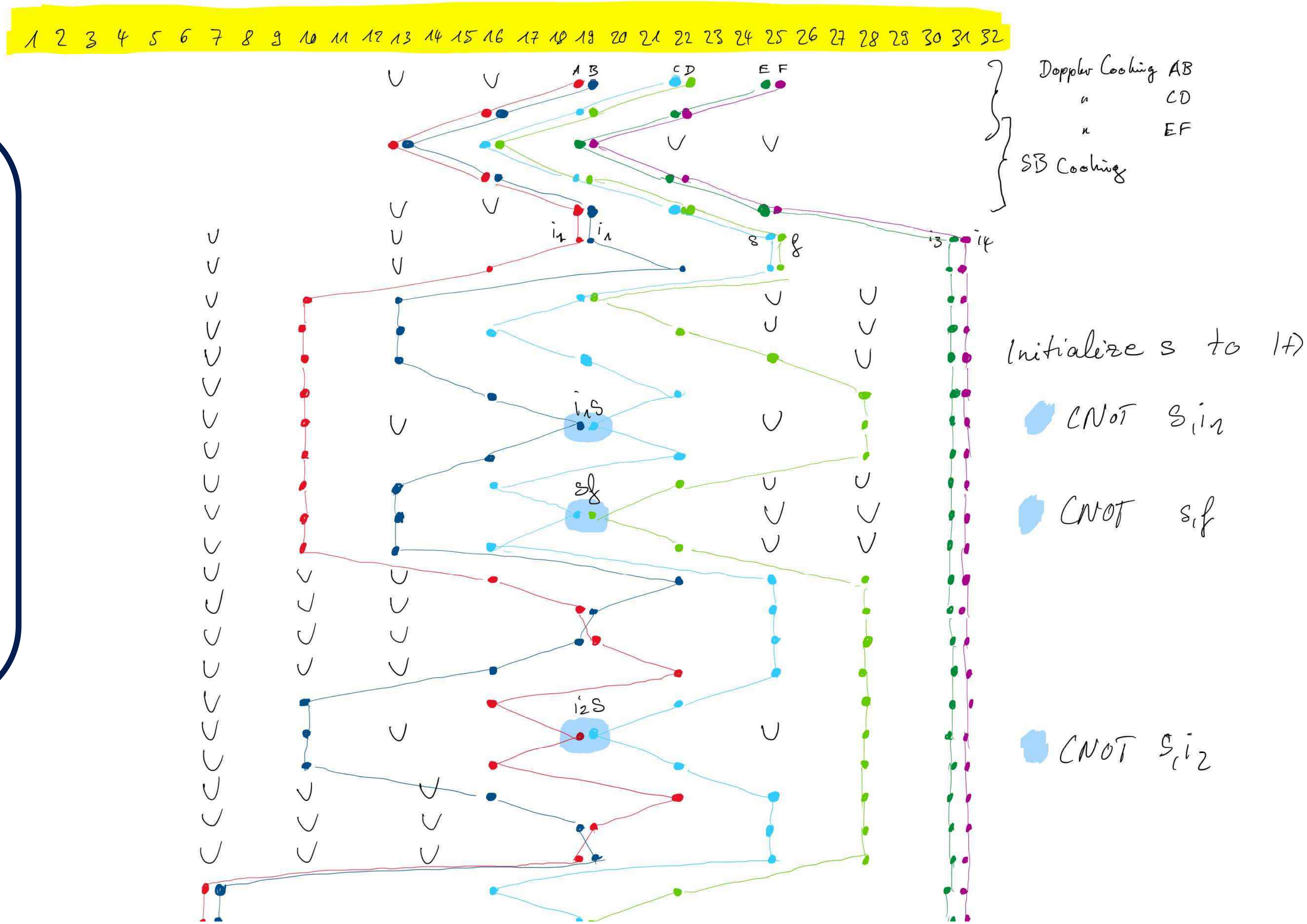

Hilder et al., *Phys. Rev. X 12, 011032 (2022)*

Fault-tolerant syndrome readout

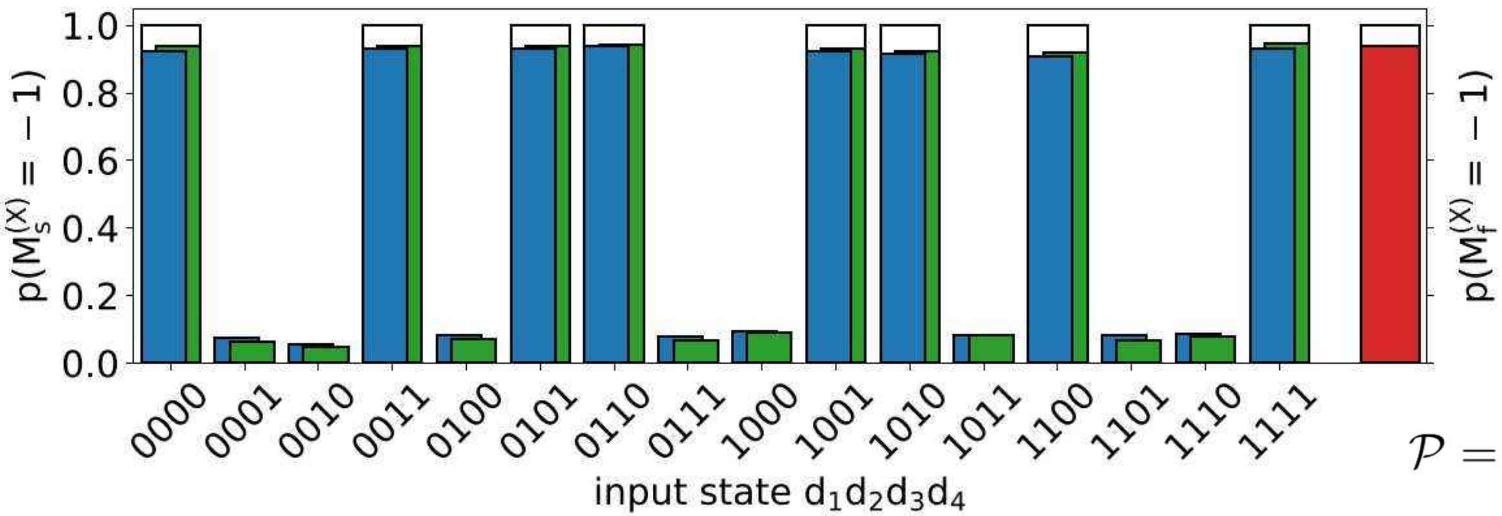

Parity readout fidelity:

$$\mathcal{P} = \frac{1}{2}\left[p(M_s^{(X)} = -1 \mid P_{in} = +1) + p(M_s^{(X)} = +1 \mid P_{in} = -1)\right]$$

- Single shot fidelity P=92.3(2)% [blue]
- Flag raised 6.3(2)%
- Post-selection on "flag not raised" [green] P=93.2(2)%
- Improvement by 4.5 σ

Egan et al., Nat. 598, 281 (2021), Postler et al, Nature 605, 675 (2022), Ryan-A. et al, Phys. Rev. X 11, 041058 (2021), Debroy et al, Phys. Rev. Lett. 127, 240501 (2021), Ryan-A. et al, arXiv:2208.01863

Error injection

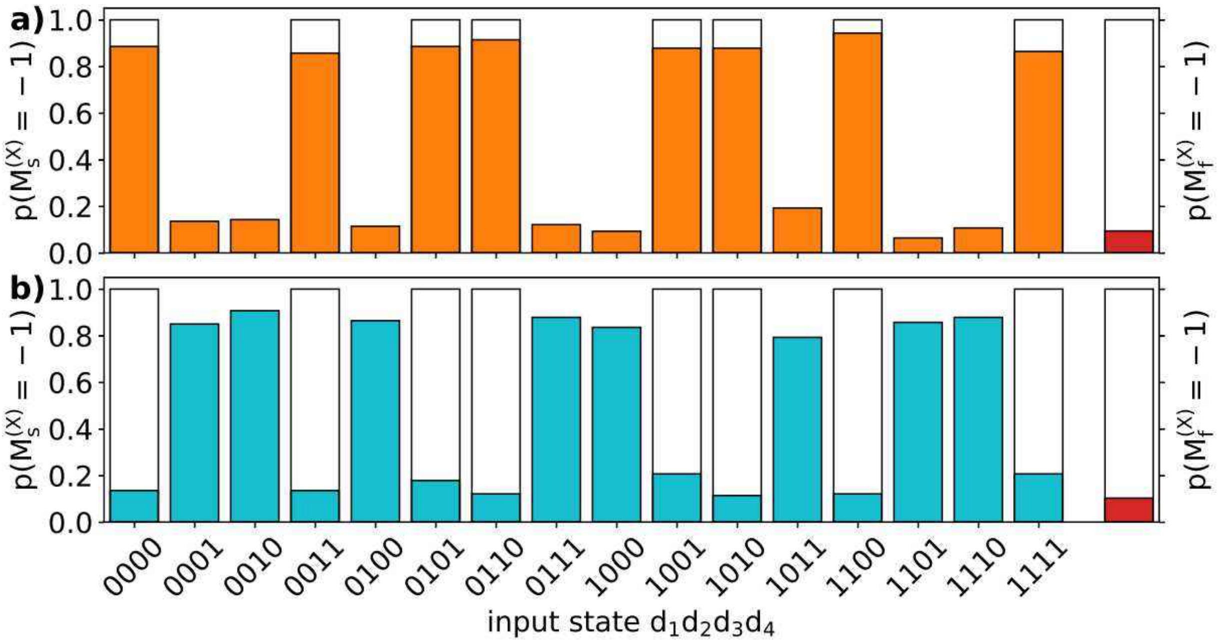

Hilder et al., Phys. Rev. X 12, 011032 (2022)

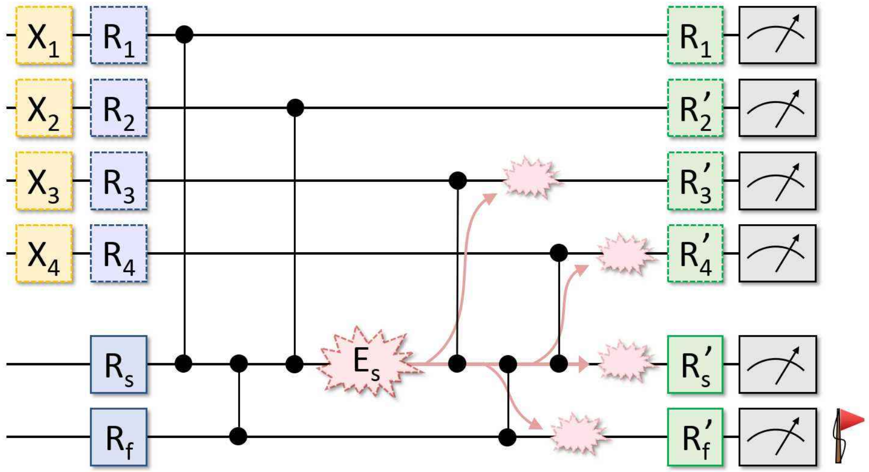

Hook-errors

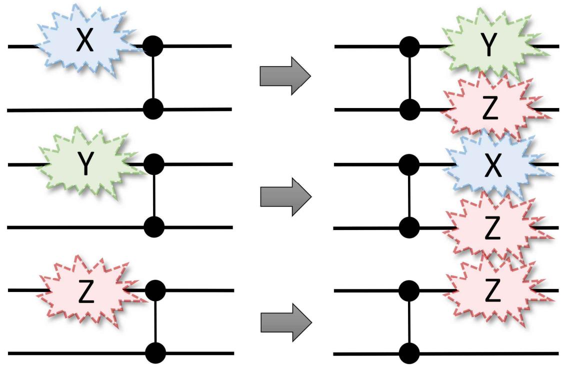

- ❑ Insert X or Y error on syndrome
- ❑ 90.6(6)% or 88.3(7)% error detection rate

Ryan-A. et al, arXiv 2107.07505
Debroy et al, arXiv 2105.05068

Hilder et al., *Phys. Rev. X 12, 011032*

Time budget

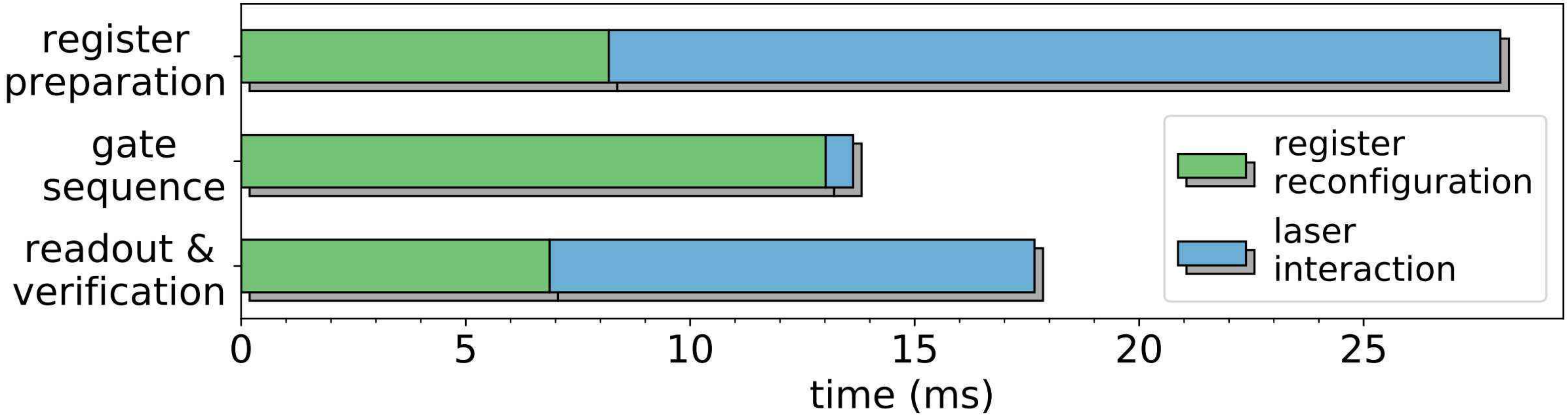

- 10% of time used for quantum algorithm

Lesson learned: Save time and be faster!

IQuAn - Architecture

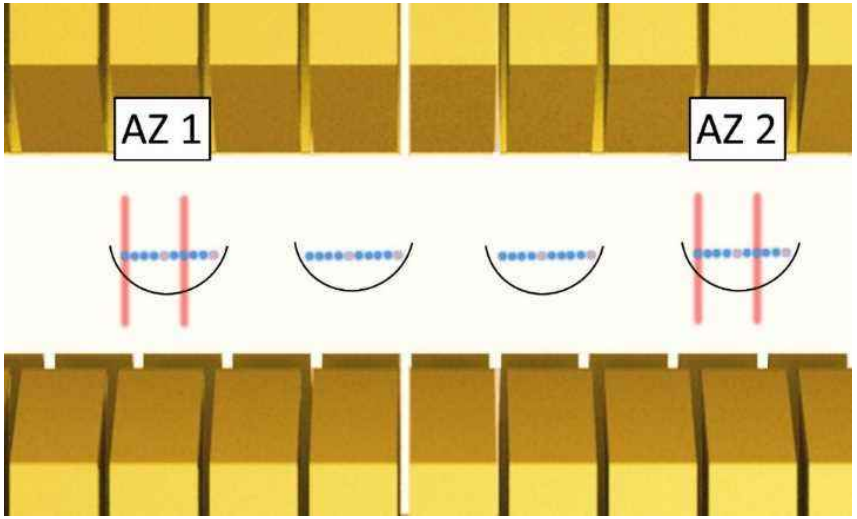

- ❑ Multiple zones for individual optical addressing for gates
  combined with
- ❑ Reconfiguration of registers, 50 ...100
- ❑ Paralell excecution of gates and reconfiguration

- ❑ Scalable, industry standard optical and electrical control units
- ❑ HPC connection

- ❑ Funding started 2021

Bundesministerium
für Bildung
und Forschung

Levels of conncetivity for scalable architecture

EVAQS, konneQt

- Level zero: ion qubits couple via common vibration, optical addressing ions
- Level one: combine this with transports of ions in segmented traps, operating multiple optical addressing zones
- Level two: combine this with optical interconnects via high N.A. or fibre optics, alternatively, junctions, ion shuttles in between different trap regions

Stopp, et al, Qu. Sci. Techn. 7 034002 (2022)

Takahashi, et al, PRL 124, 013602 (2020)

Krutyanskiy, et al, PRL 130, 050803 (2023)

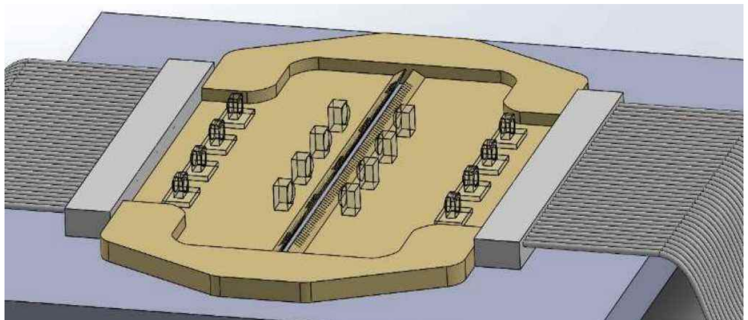

integration of optics conn.

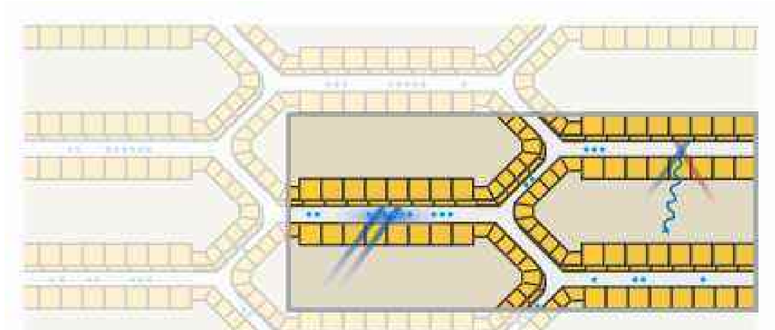

Integration of junction struct.

Hardware components & control modules

- ❑ SLE Ion traps / 40 segments
- ❑ High optical access Ti-UHV vessel
- ❑ 3-layer μ-metal shield
- ❑ Laser racks, fiber coupled
- ❑ Light processing units
- ❑ DC and RF multichannel AWGs

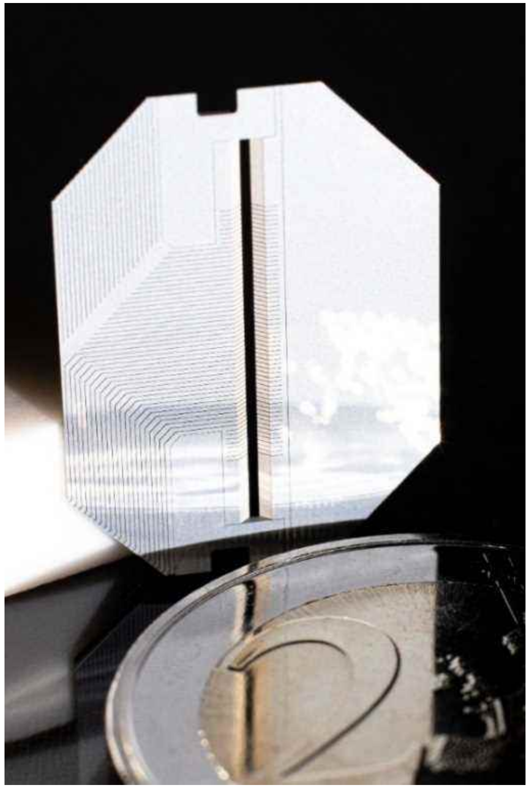

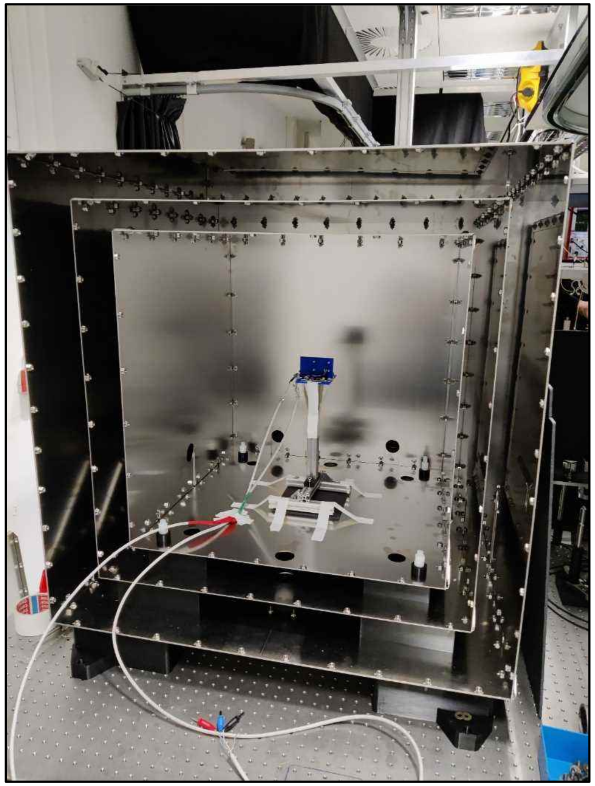

TRAPS cleanroom

- SLE trap fab.
- Sputter, dicer, asher
- Wet bench,
- Microscopes, wire bonder

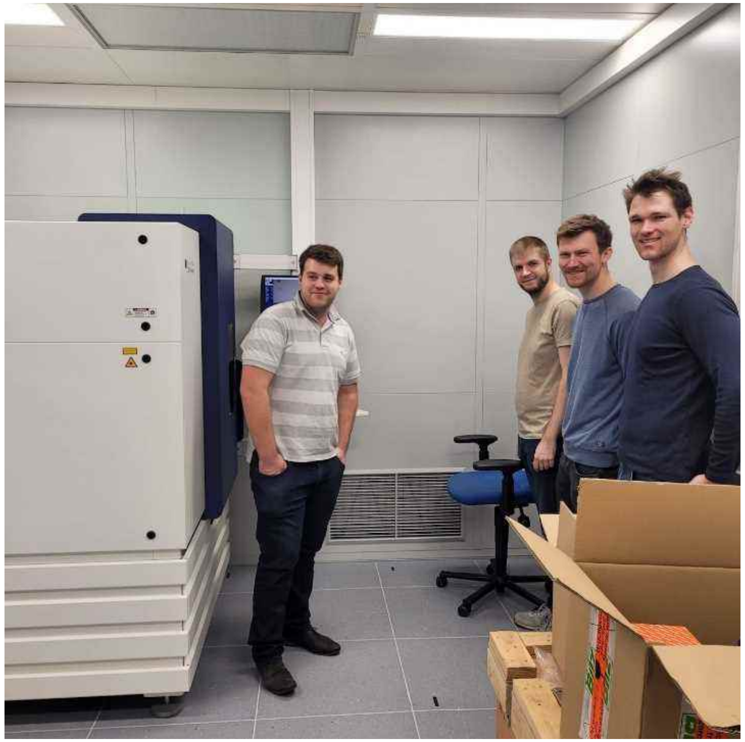

See also: Ragg et al, Rev. Sci. Instr. 90, 103203 (2019)

SLE written structures

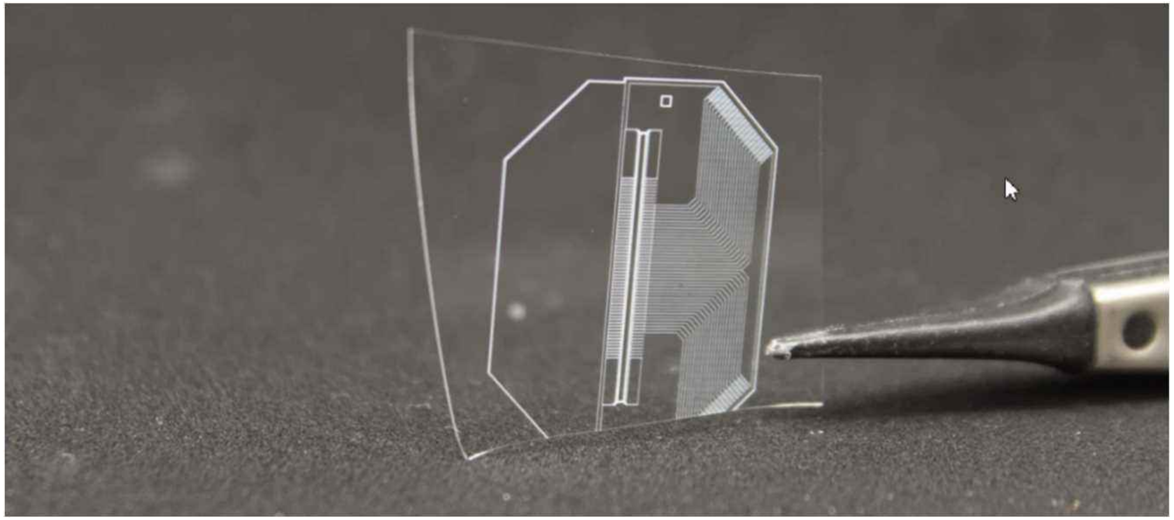

See also: Ragg et al, Rev. Sci. Instr. 90, 103203 (2019)

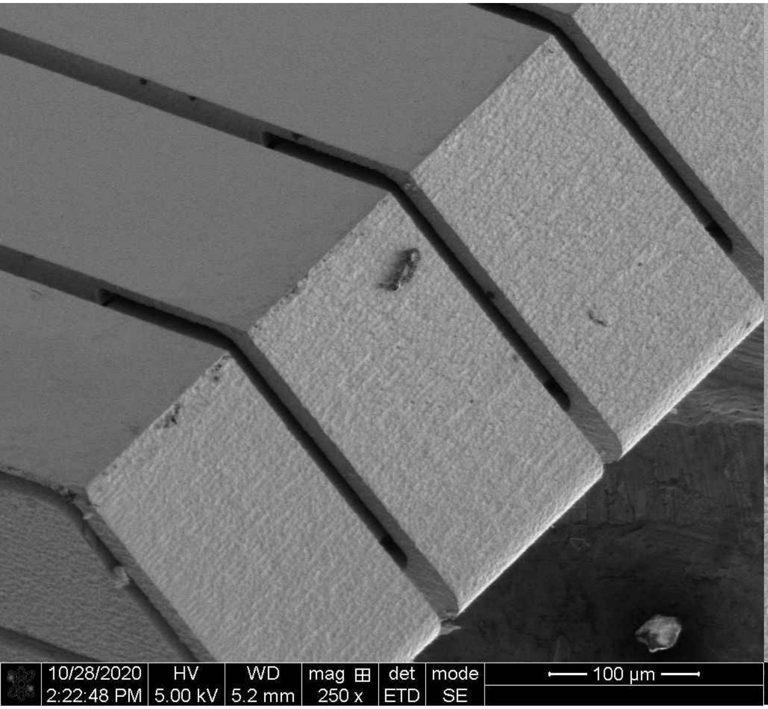

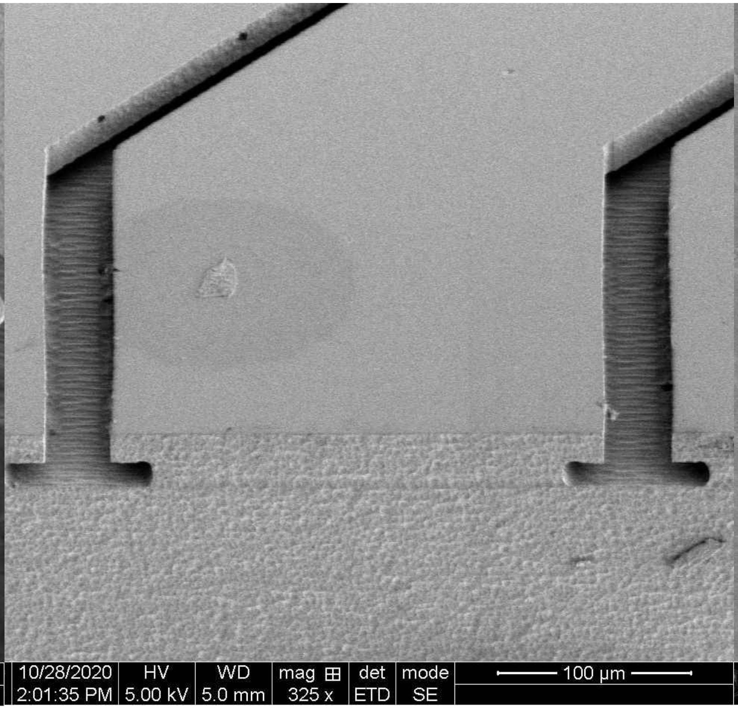

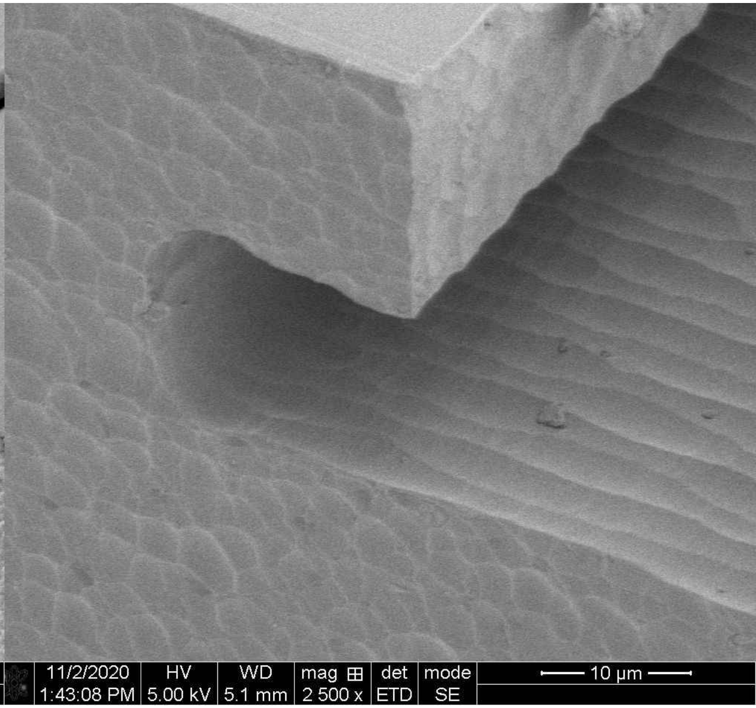

Reliable optical qubit control, get free space in the lab

Rackmount laser units

- Laser sets for $^{40/44}Ca$
  Sympathetic cooling of radial modes
- LPUs: (rack-based light processing units)
  - for switching of light
  - FM-EOMs
  - automatic fiber coupling
  - outstanding stability
- Frequency locking by wavemeter and ultra stable cavities (rack-based)

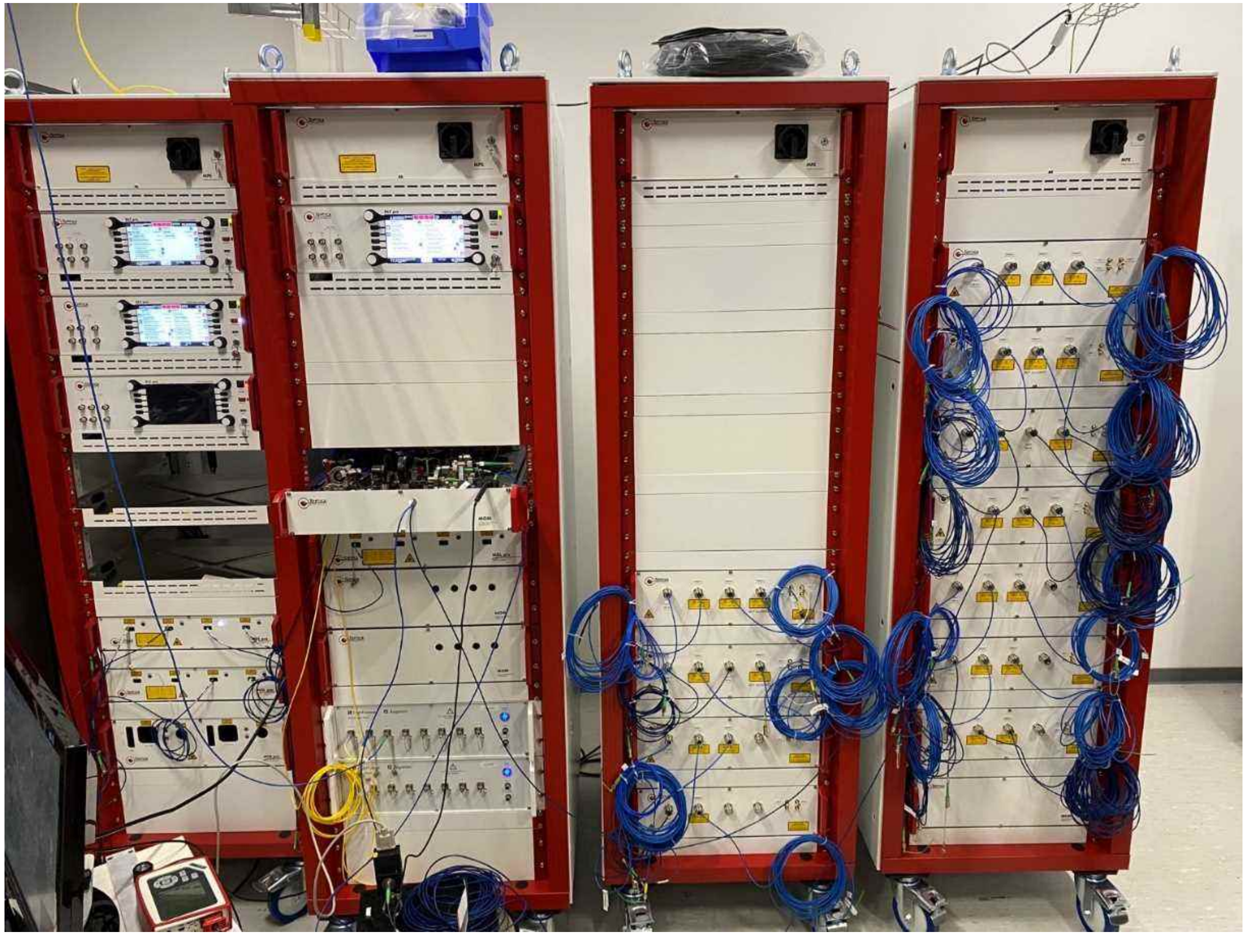

Quantum computer control room

Software stack

User Frontend (Website, Pennylane, Mogon)

↕

Quantum Circuit Compiler

↕

Operation Sequence Manager

↕

MCP.exe ⇄ Hardware

↕

Lab user / maintainer

User interaction via

- ❑ Drag & Drop Circuit Builder
- ❑ OpenQASM
- ❑ Pennylane & Qiskit
- ❑ HPC Mogon II connection
- ❑ Integration of user management and database

Quantum circuit optimizer

- Converts quantum circuit into native gate set
- Optimizes the quantum circuit with respect to shuttling overhead and number of gates
- SWAP elimination
- Different degrees of optimization possible
- Macro-matching & phase tracking
- Gate count reduction by 3.6 (as compared to Pytket)
- Similar performance as AQT compiler, but for shuttle-based situation

$$\mathcal{M} = \{\mathrm{R}(\theta, \phi), \mathrm{Rz}(\phi), \mathrm{ZZ}(\theta)\}$$

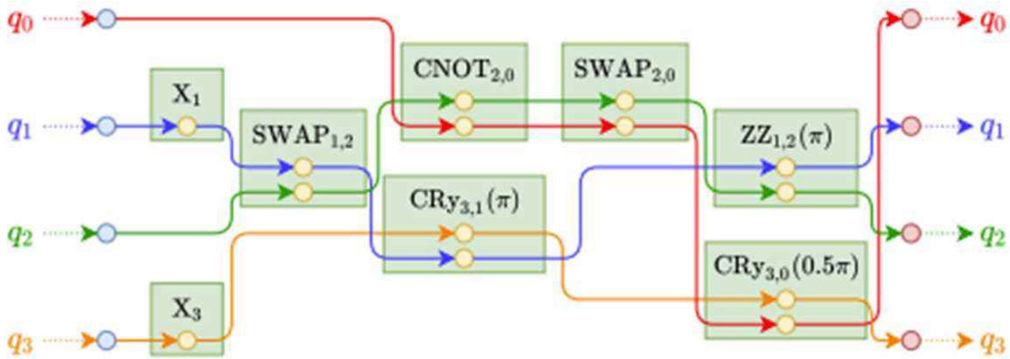

Fig. 4: Example of a graph representation of a quantum circuit with four qubits. The circuit contains gates not being part of the restricted native gate set $\mathcal{N}$.

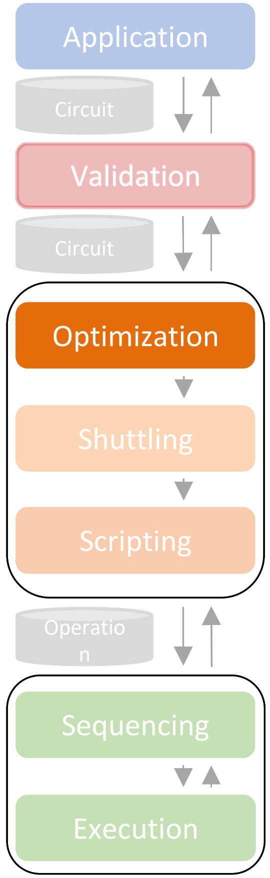

Kreppel, et al. Quantum Circuit Compiler for a Shuttling-Based Trapped-Ion Quantum Computer. arXiv: 2207.01964

Circuit optimizer, acting with symbolic gates

- Define and compile circuits including symbols
- Compilation only once
- Executions with different sets of parameters
- Same sequence in each repetition, important in VQE

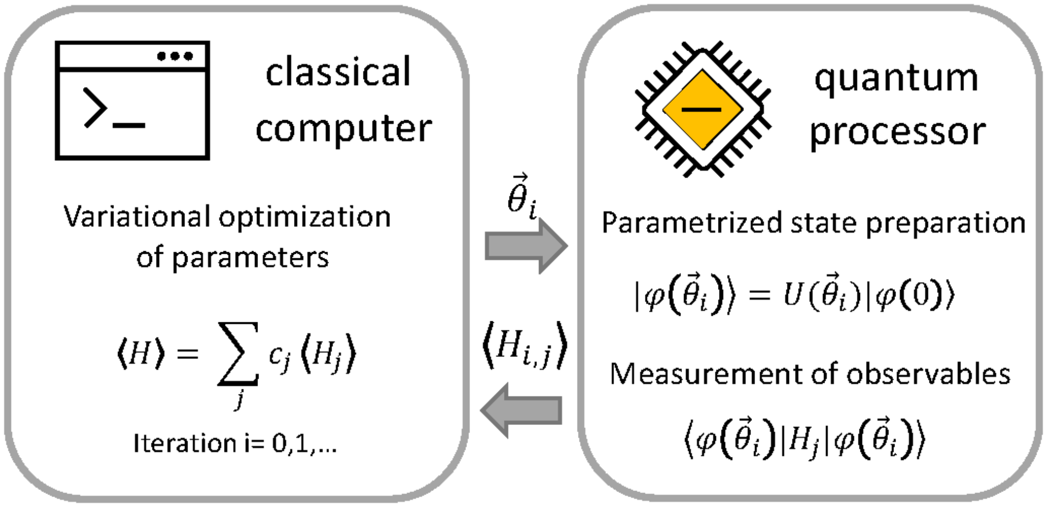

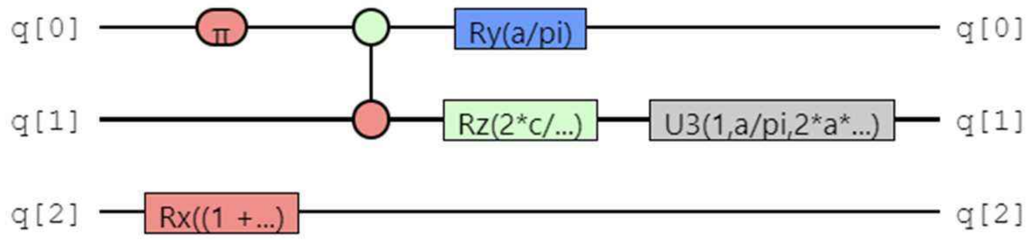

Define parameter set:
{a: … ,b: … ,c: … }

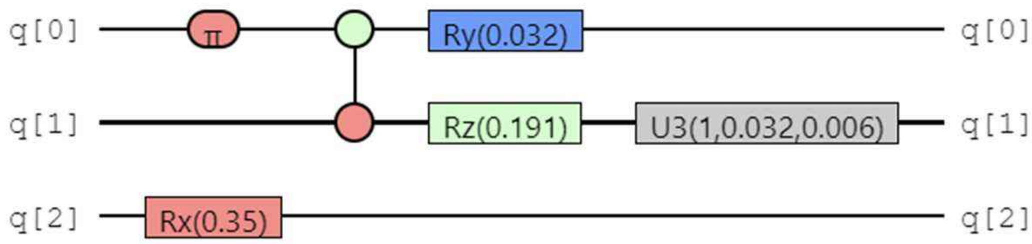

Shuttling compiler

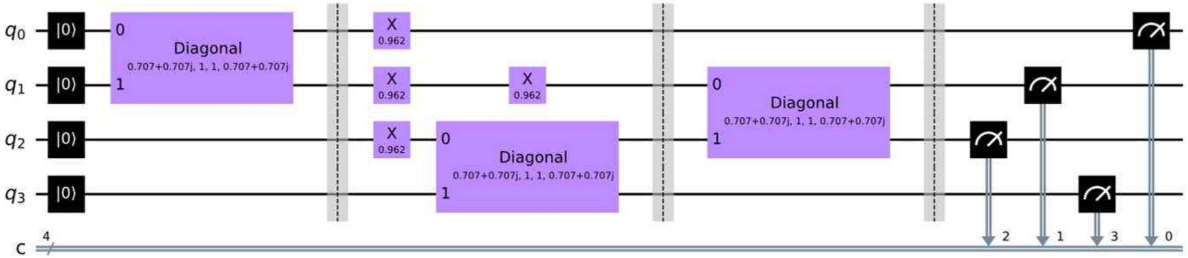

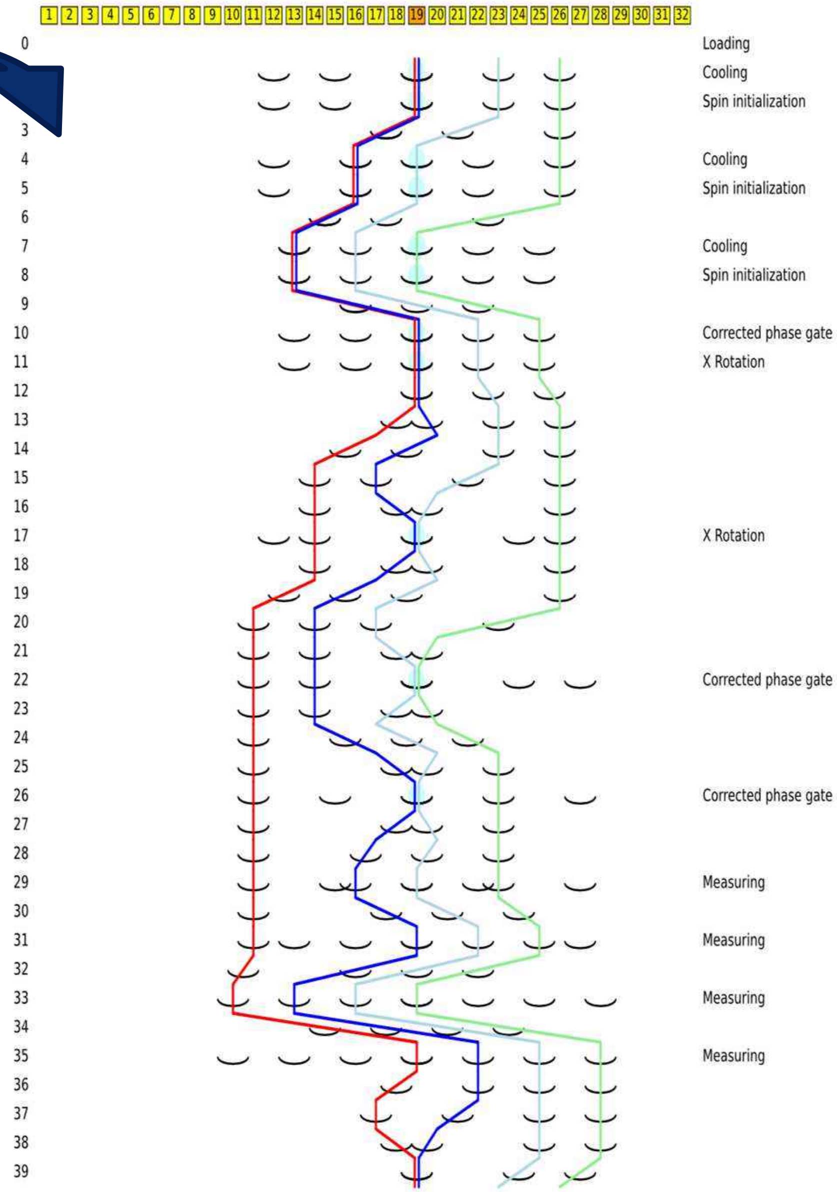

- Finds an initial mapping from qubits to ions heuristically
- Basic operations: translate, separate/merge, swap
- Currently: operations executed in the Laser Interaction Zone (LIZ) on ≤2 ions

Wagner, Master thesis (2022), Durandau et al, arXiv:2207.01964, published

Combine addressing and reconfiguration

- Drastic reduction of reconfiguration overhead
- Requires controlled multi-ion separation
- Remote reconfiguration operations

- Shuttle reduction: factor 5
- Separation reduction: factor 3
- SWAP reduction: factor 3

- IQuAn architecture

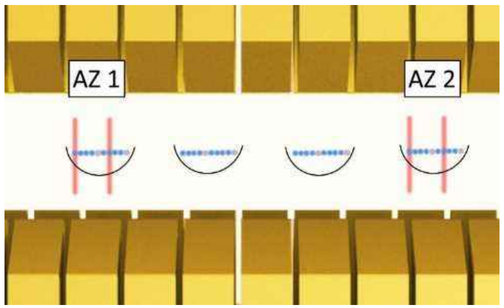

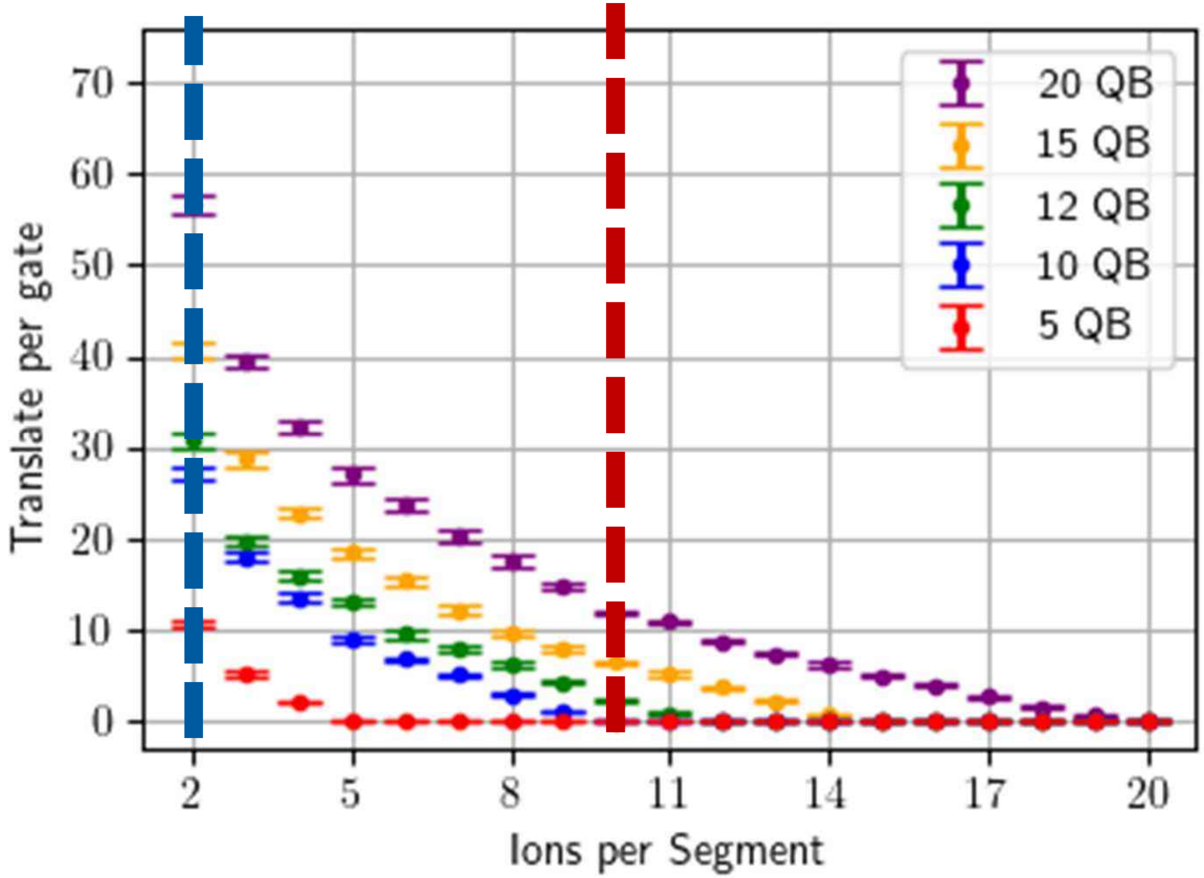

Mid-circuit qubit detection

- Illumination 729nm/854nm and 393nm photon detection
- Pros: no background UV light, no Doppler heating, little reabsorption, low qubit crosstalk

Applications:
quantum error correction, measurement-based QC
branching decisions, …..

Verde et al, to be published

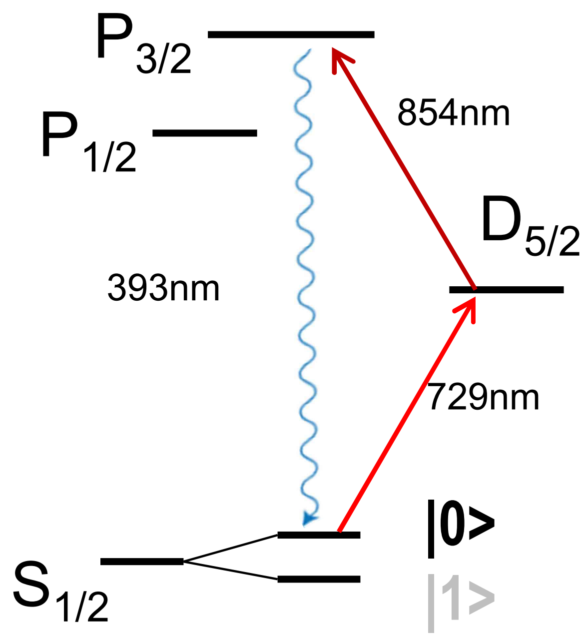

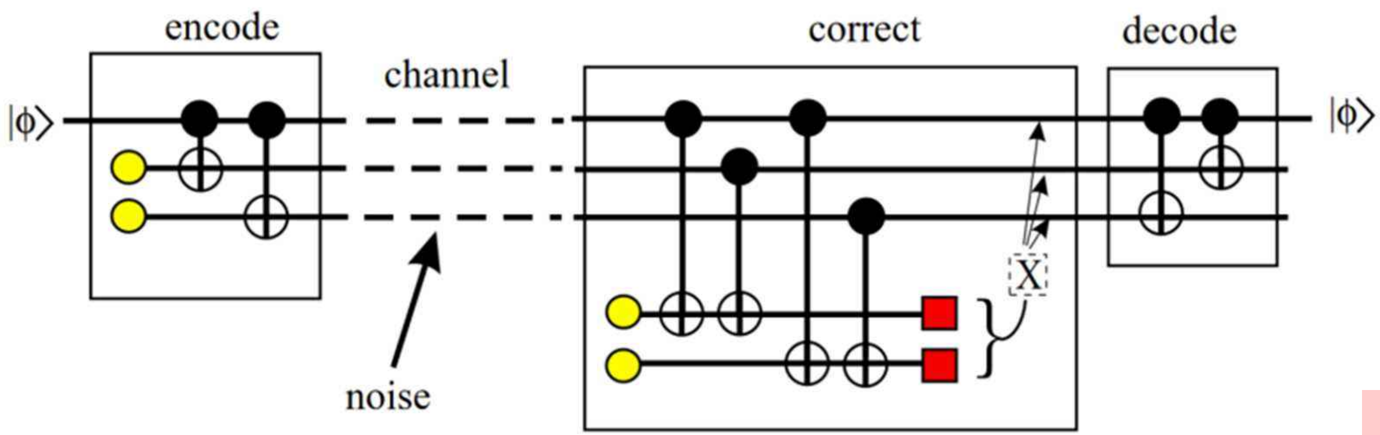

Graham et al, arXiv:2303.10051
Motlakunta et al, arXiv:2306.03075

Hilder et al., Phys. Rev. X 12, 011032 (2022)

Stahl et al.

Realtime conditional reconfiguration operations

- FPGA SoC redesign
- PMT counter and thresholding on fmAWG
- Real-time decision logic

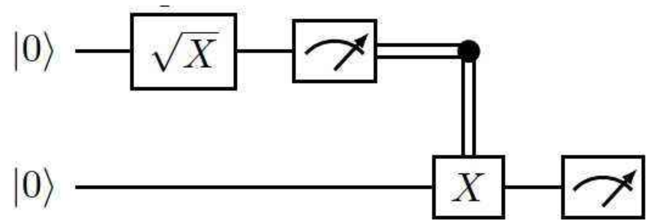

Proof-of-principle: conditional qubit init. by *conditional shuttling* to laser-interaction zone

Furthermore:
Daemonic ergotropy with enhanced work extraction from quantum correlations

Francia, Goold, Plastina, Pernostro, npj quant. Inf. 3, 12 (2017)

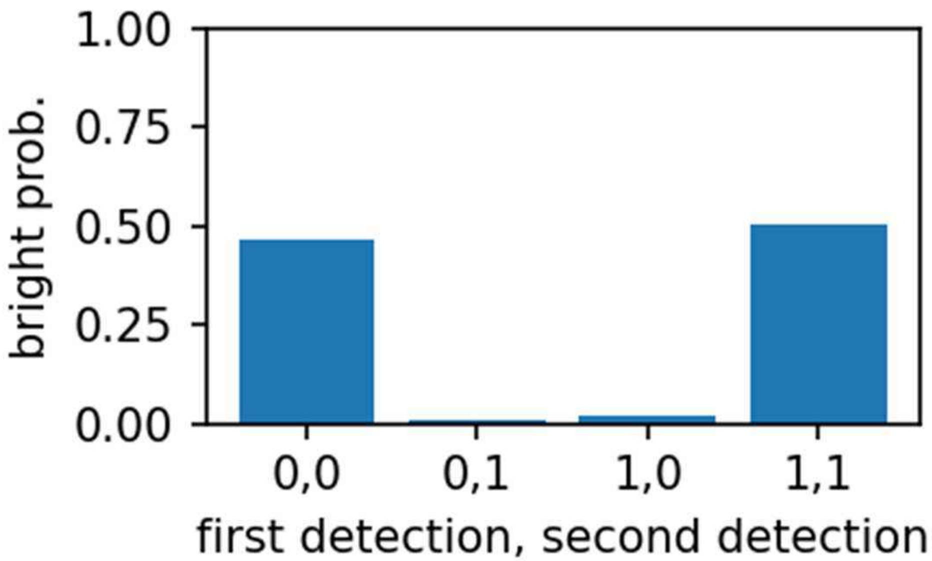

IQuAn / ATIQ access

https://www.iquan.de

IQuAn

Bundesministerium für Bildung und Forschung

Consortium:
Ionen-Quantenprozessor mit HPC-Anbindung (IQuAn)

JOHANNES GUTENBERG UNIVERSITÄT MAINZ

JÜLICH Forschungszentrum

Fraunhofer ILT
Fraunhofer-Institut für Lasertechnik ILT

Fraunhofer IOF
Fraunhofer-Institut für Angewandte Optik und Feinmechanik IOF

TOPTICA PHOTONICS

AKKA PASSION FOR TECHNOLOGIES

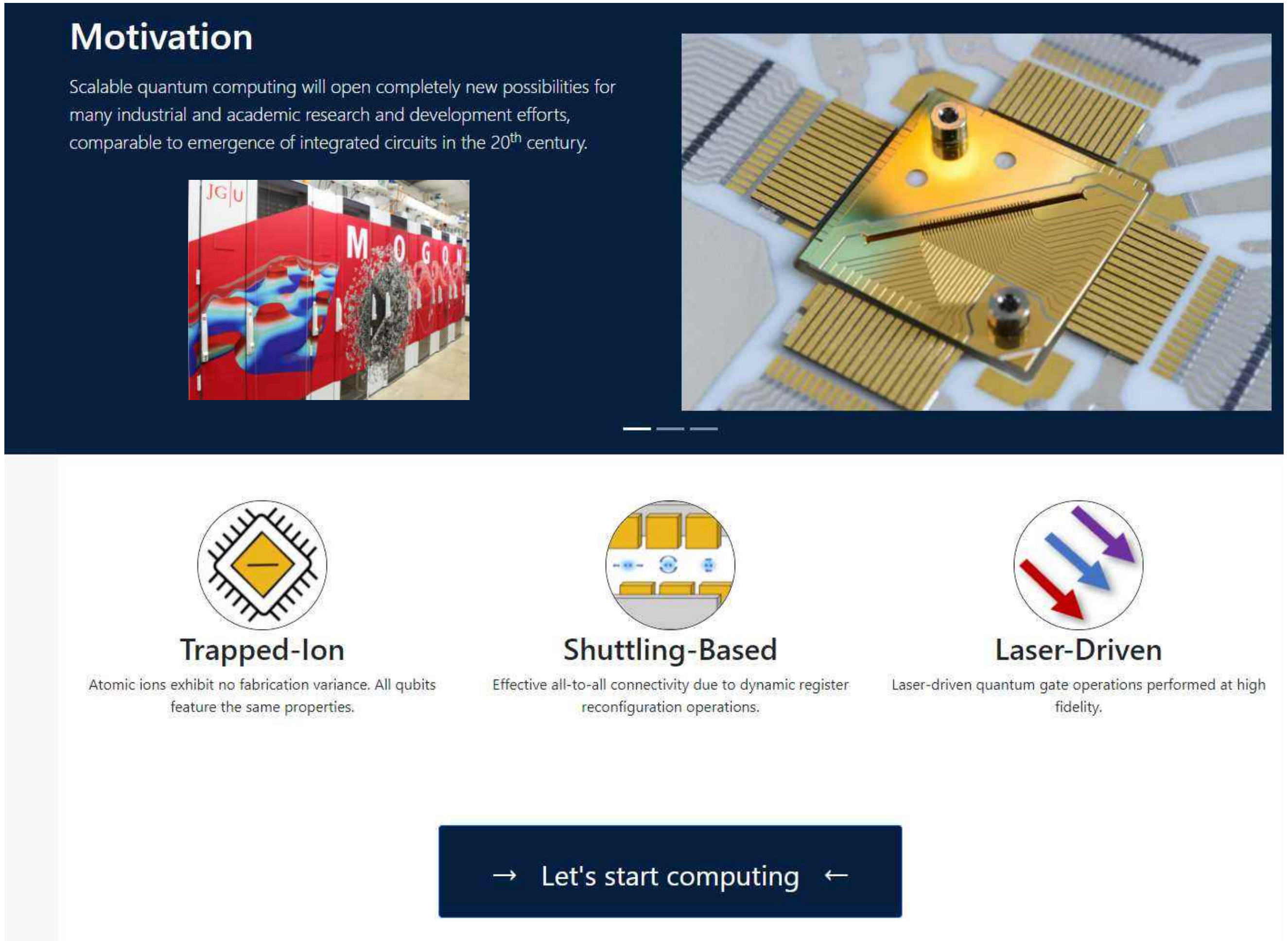

Applications and cooperations

VQE - Hybrid Variational Quantum Eigensolver

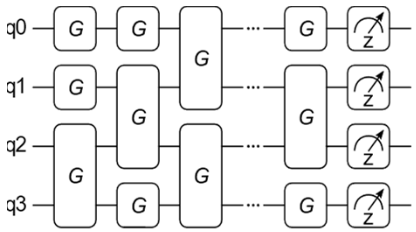

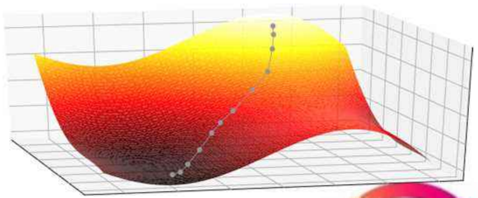

Determine the ground state of a molecule

ParityQC Architecture

Map optimization problem to
parallelizable design of four-qubit interactions

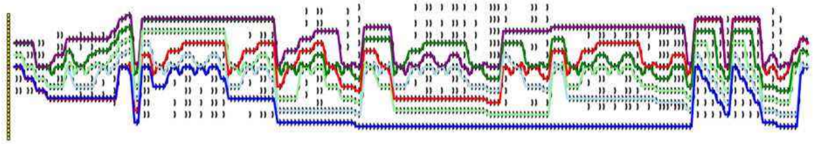

VQS for High-Energy Physics K. Jansen, DESY

Variational Quantum Simulation of Multi-Flavor
Schwinger Model

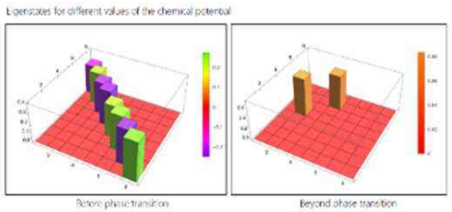

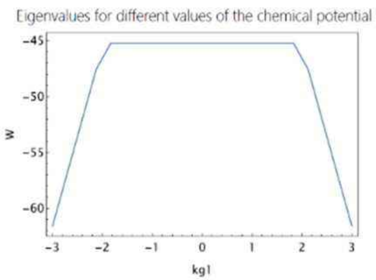

Beyond NISQ T. Monz / M. Müller

Ongoing work on:

- QEC – Quantum Error Correction
- QAE – Quantum Auto Encoder
- Logic operations with logic qubits

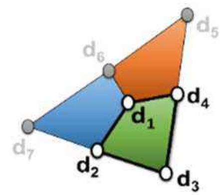

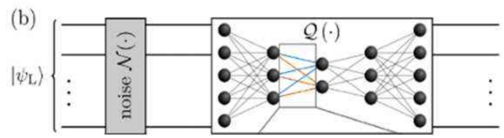

Bundesministerium
für Bildung
und Forschung

Mainz Quantum Computer Experiments

IQuAn

|ATIQ⟩

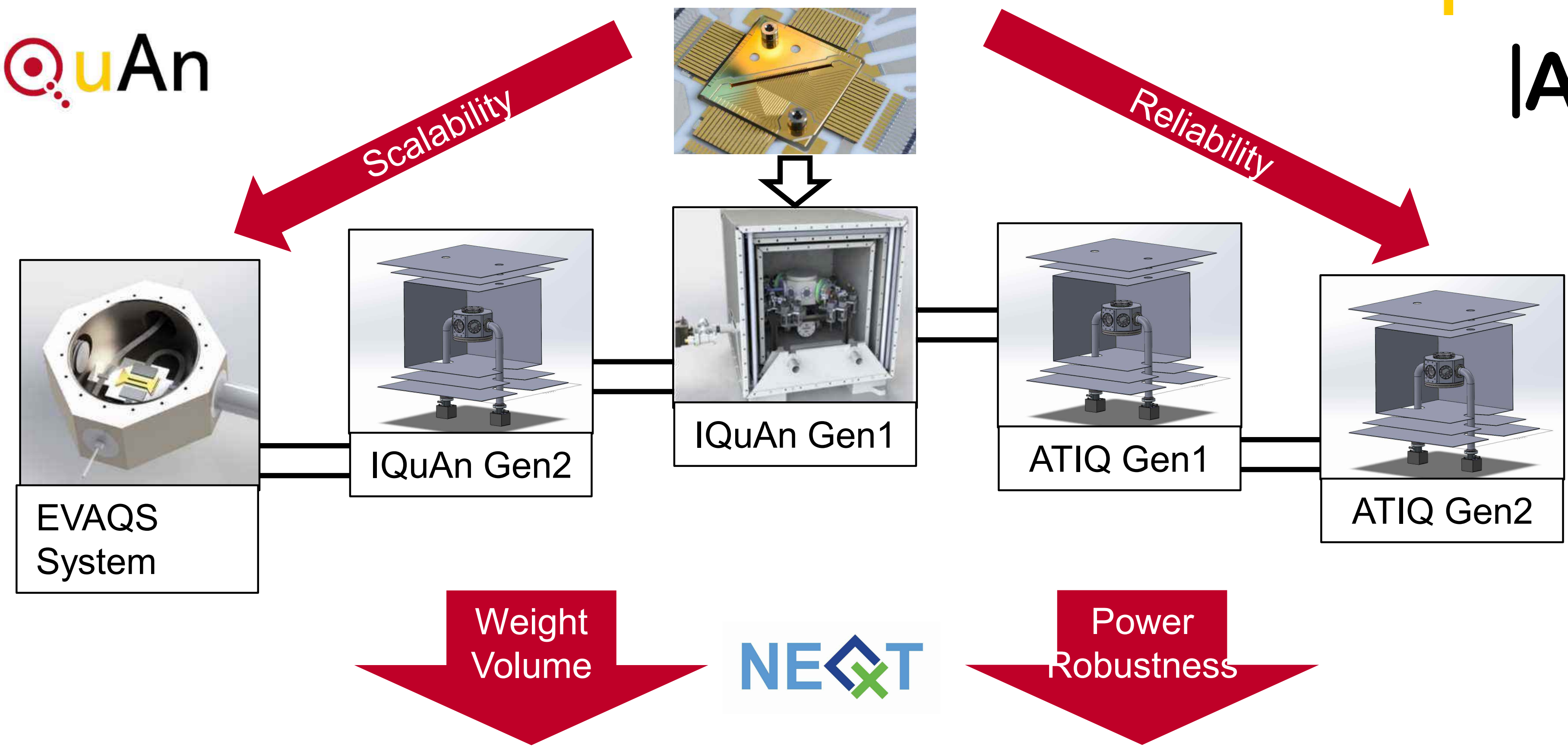

commercializing Quantum Computer

Startup NEQXT

- Fully integrated ion processor modules, fibre coupled
- Scalable to > 100 fully connected qubits
- Entire software stack & used case examples

https://neqxt.org/

- Compact, modular FPGA controlled electronic units
- Clean room for custom SLE fabrication

Key figures in trapped ion QC

long-range Coulomb interaction

- ❑ Single shot read-out of spin state better than $1 - 10^{-4}$
- ❑ Single gate fidelity better than $1 - 10^{-4} \ldots 10^{-5}$
- ❑ Two qubit gate fidelity $1 – 10^{-3} \ldots 10^{-4}$
- ❑ Two-qubit gate operation times ~ 30 … 100 µs

Ion qubit entanglement is relatively slow

Rydberg properties

Zhang et al, Nat. 580, 345 (2020)
Saffman, Walker, Mölmer, RMP 82, 2313 (2010)

- ❑ **Rydberg dipole blockade**
- ❑ **Rydberg polarizability - state-dependent effective ion mass**

Vogel et al, PRL123, 153603 (2019)
Han et al., (2023)

Join advantages for ion trap qubits
with Rydberg excitations and interactions

Rydberg excitation of a single ion

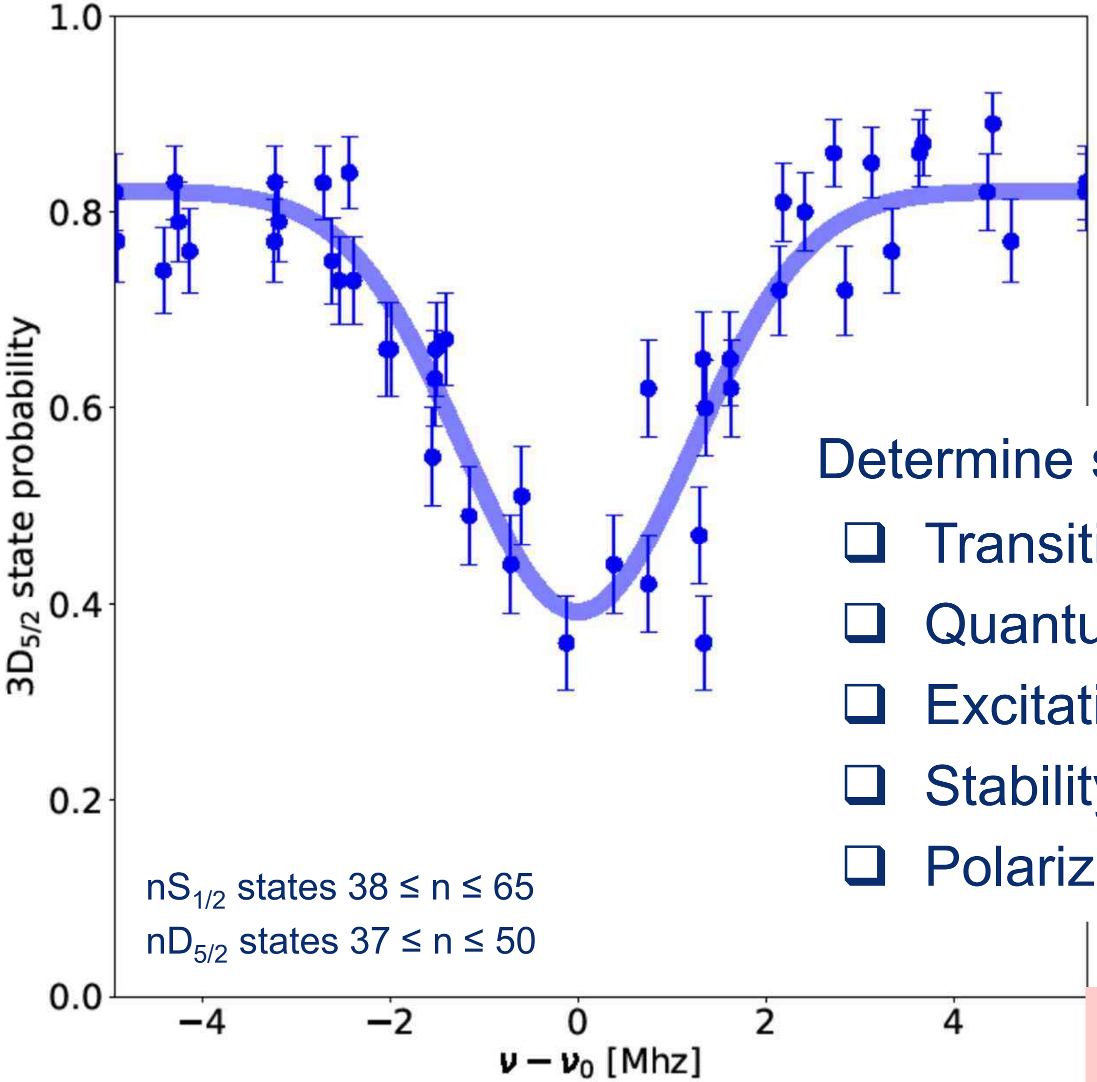

Determine spectroscopically

- ❑ Transition energy
- ❑ Quantum defect
- ❑ Excitation strength
- ❑ Stability in trap
- ❑ Polarizability

Niederländer et al, NJP 25 033020 (2023)

Andrijauskas et al., PRL 127, 203001 (2021)

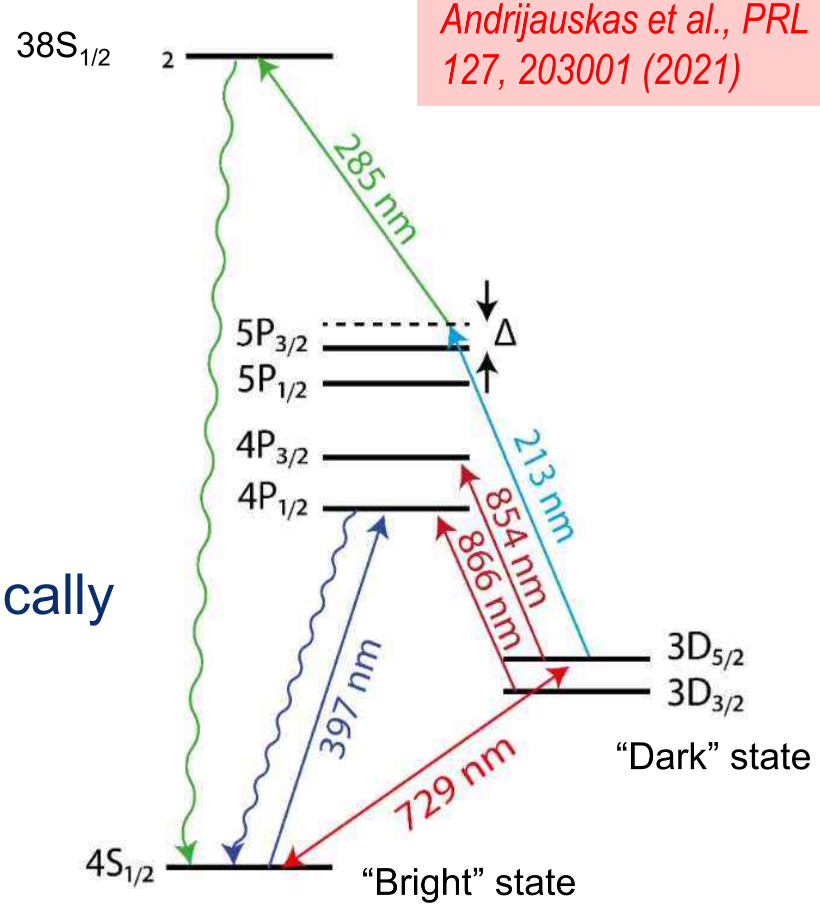

Schmidt-Kaler et al, NJP 13, 075014 (2011)
Feldker et al, PRL 115, 173001 (2015)
Higgings et al, PRX X 7, 021038 (2017)
Zhang et al, Nature 580, 345 (2020)

Polarizability → Trap frequency change

- Radial electr. field gradient much higher as axial

$\gamma_{DC} = 4.69 \times 10^6\ \mathrm{V/m^2}$
$\gamma_{RF} = 3.33 \times 10^8\ \mathrm{V/m^2}$

$$\omega_x = \sqrt{\frac{2e^2\gamma_{\mathrm{RF}}^2}{M^2\Omega_{\mathrm{RF}}^2} - \frac{2e\gamma_{\mathrm{DC}}(1+\epsilon)}{M} - \frac{2\mathcal{P}\left(\gamma_{\mathrm{RF}}^2 + \gamma_{\mathrm{DC}}^2(1+\epsilon)^2\right)}{M}}$$

$$\omega_y = \sqrt{\frac{2e^2\gamma_{\mathrm{RF}}^2}{M^2\Omega_{\mathrm{RF}}^2} - \frac{2e\gamma_{\mathrm{DC}}(1-\epsilon)}{M} - \frac{2\mathcal{P}\left(\gamma_{\mathrm{RF}}^2 + \gamma_{\mathrm{DC}}^2(1-\epsilon)^2\right)}{M}}$$

$$\omega_z = \sqrt{\frac{4e\gamma_{\mathrm{DC}}}{M} - \frac{16\mathcal{P}\gamma_{\mathrm{DC}}^2}{M}} \quad .$$

- Choose n → P(nS)
- Radial: 1.64MHz – 33.8kHz
  Axial : 1.07MHz – 47Hz

$P(49S_{1/2}) = 1.3 \times 10^{-30}\ \frac{C \cdot m^2}{V}$

	|00>	|01>	|10>	|11>
Rocking (MHz)	1.239	1.216	1.216	1.194
Rad. CM mode (MHz)	1.637	1.621	1.621	1.604

- Close the phase space trajectories with the properly chose kick sequence and get the right phase area – kick it back to the origin

Exploring the E-field in the trap

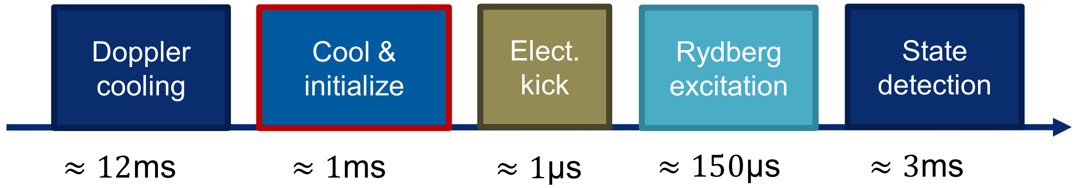

- ❑ Cool ion near ground state
- ❑ Generate coherent state of ion radial motion
- ❑ Sense interaction with electric field

- ❑ Observe shift due to polarizability

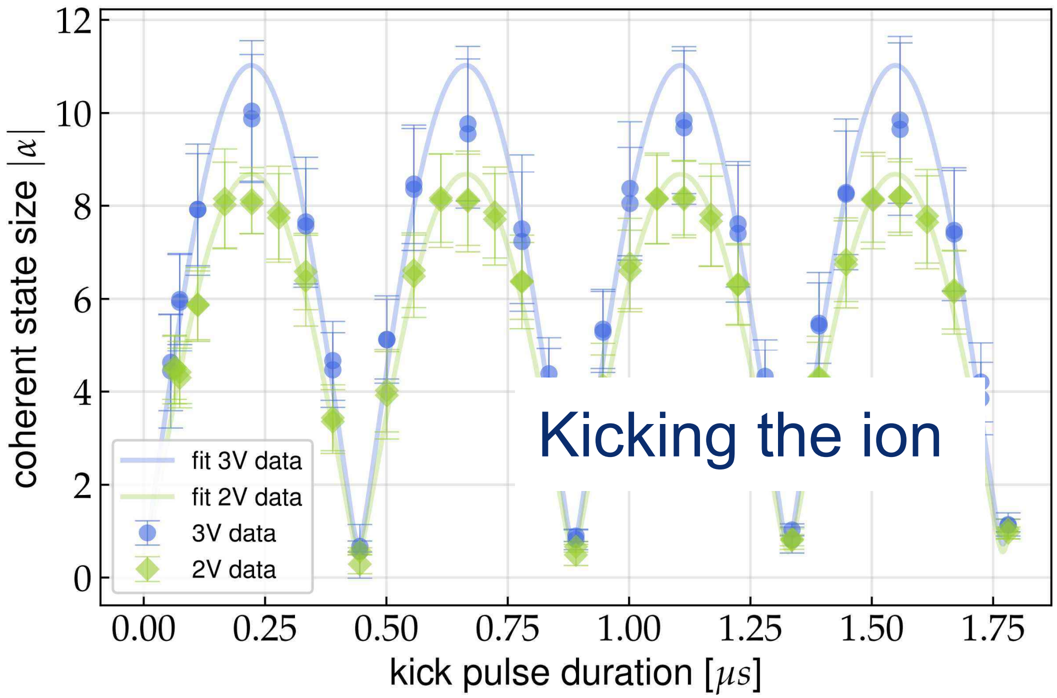

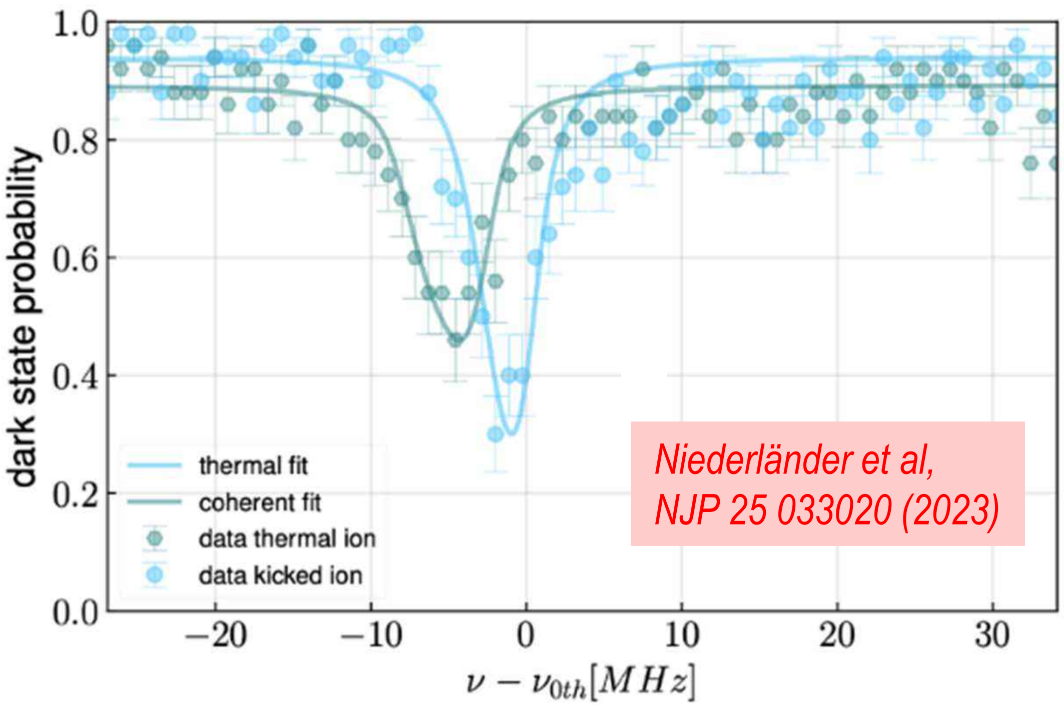

Kicking ion crystal for entanglement

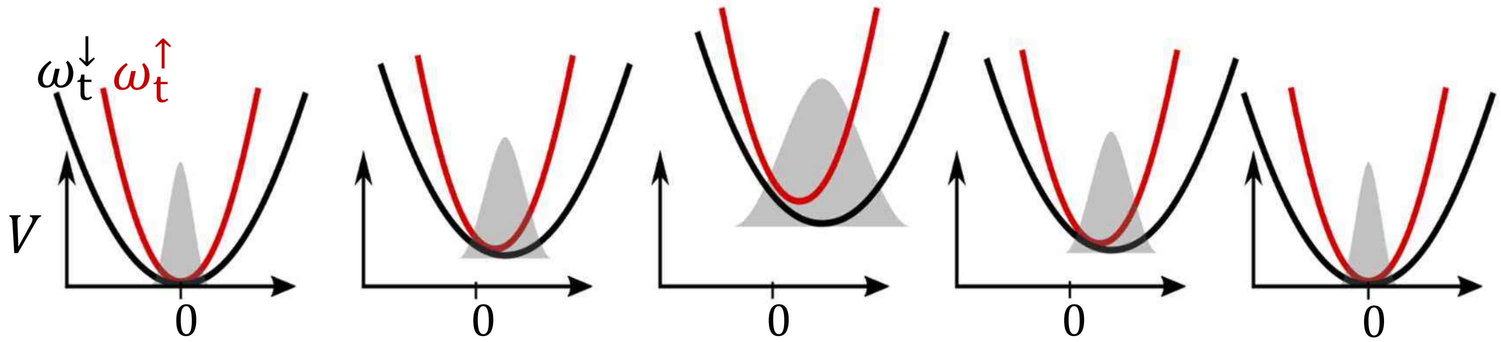

Ripol et at., Phys. Rev. A 71, 062309 (2005), Steane, New J. Phys. 16, 053049 (2014), Schäfer et at, Nat. 555, 75 (2018), Shapira et al. Phys. Rev. A 101, 032330 (2020)

- ❑ Excite a superposition of $D_{5/2}$ (↓) and Rydberg state (↑)
- ❑ Apply electric kick (i)
- ❑ Rydberg polarizabilty results in spin-dependent potential
- ❑ Kick back (ii)
- ❑ Observe geometric phase

To do:

- ❑ Robustification against δV and $\delta\tau$
- ❑ all-to-all in N=10 ion crystal

Vogel et al, PRL123, 153603 (2019)

Bao et al, (2023)

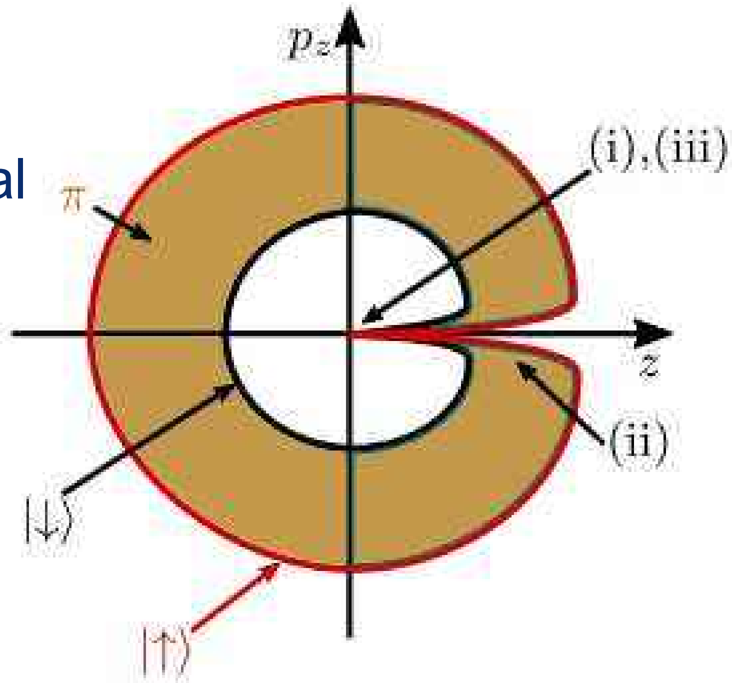

Conclusion – Rydberg excitations of trapped ions

- New platform is established experimentally
- Spectroscopy groundwork done
- Polarizability tuning by MW dressing and trap E-fields
- Pathways towards sub-μs high fidelity gate operation
- Rydberg excitations may contribute to the ion qubit toolbox

First Ryd. Ion ever: Feldker et al, PRL 115, 173001 (2015)
Fast gate proposal: Vogel et al, PRL 123, 153603 (2019)
Spectroscopy: Andrijauskas et al, PRL 127, 203001 (2021)
Rydberg ion review: Mohberi et al, Adv. At. Mol. Opt. Phys. 69, 233 (2020)

Quantum Computing Team @ JGU Mainz

Want to join?


Jonas Vogel


Daniel Pijn


Janine Hilder


Björn Lekitsch


Ulrich Poschinger


Ferdinand Schmidt-Kaler


Felix Stopp

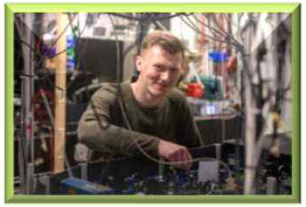
Jan Müller


Alexander Stahl


Maximilian Orth


Christian Melzer


Janis Wagner


Alexander Müller

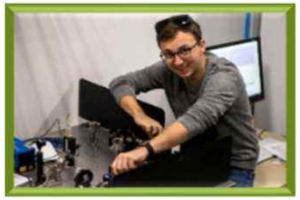
Robin Strohmaier


Daniel Wessel


Diego Olvera Millán


Andreas Conta


Sahori Jiménez


Helin Özel


Dario Moreira

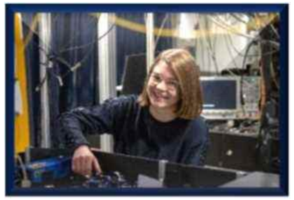
Pauline Wagner

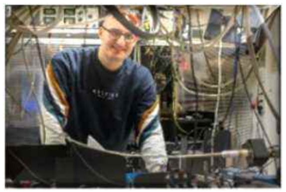
Lukas Klein

Fabian Kreppel

André Brinkmann

Quantum technologies with trapped ions @QUANTUM

www.quantenbit.de

Want to join?

Rydberg ions

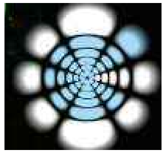

PRL 115, 173001
PRL 123, 153603
Adv. At. Mol. Opt. Phys. 69, 233
PRL 127, 203001
NJP 25, 033020

Sci. 352, 325
PRL 123, 080602
PRL 128, 110601

Ion heat engines

Universal trapped-ion Quantum Computer

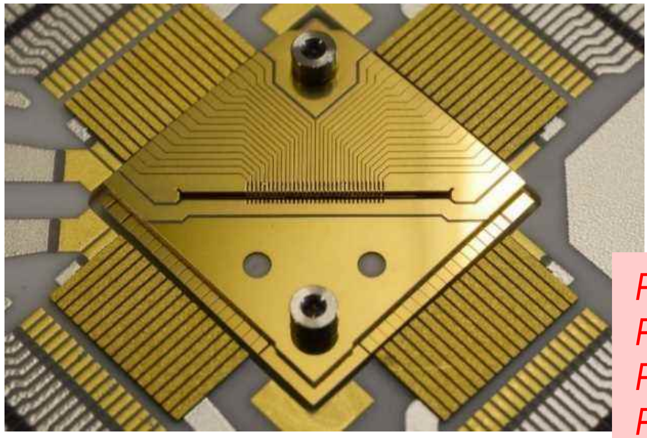

PRL 119, 150503
PRX 7, 031050
PRX 7, 041061
PRX 12, 011032

Exotic ions: $\bar{H}^+$ / Th^+

PRA 99, 023420
NJP.24, 043028
PRX Q3, 010330

PRL 116, 183002
PRL 126, 173602
PRL 127, 143602
PRR 5, 013163

Photon correlations $g^{(2)}(x,\tau)$

Single ions delivered for solid state QC

PRL 117, 043001
PRL 123, 106802
Qu. Sci.Techn.7, 034002

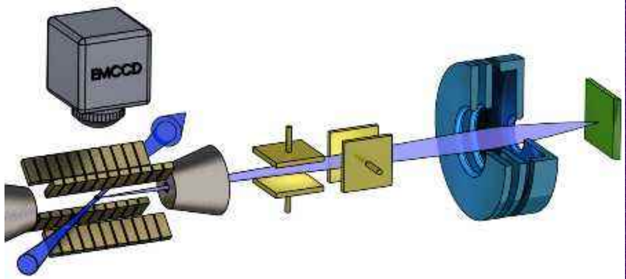

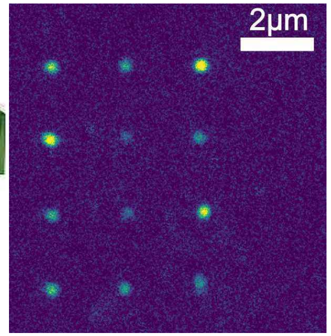

Optical angular momentum

Nat.Com. 7, 12998
PRL 119, 253203
JOSA B 36, 565
PRL127, 143602
PRL 129, 263603

Spin-echo gate operation

- perform spin echo for spin-asymmetric error sources
- minimize residual displacement with phase of 2nd pulse
- back to initial phonon state

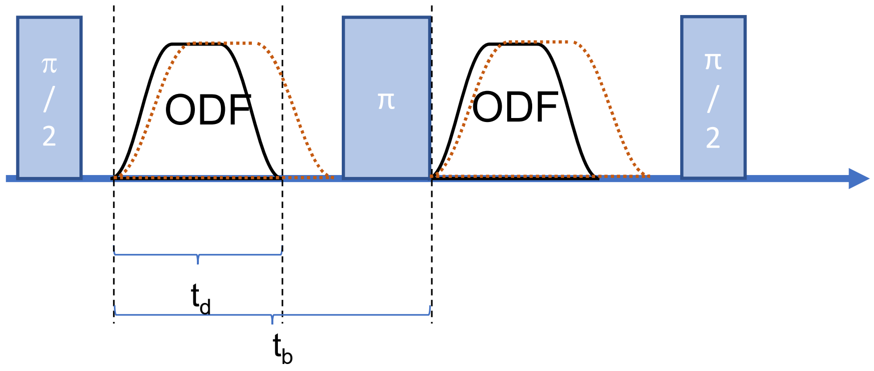

robust in phase and in duration

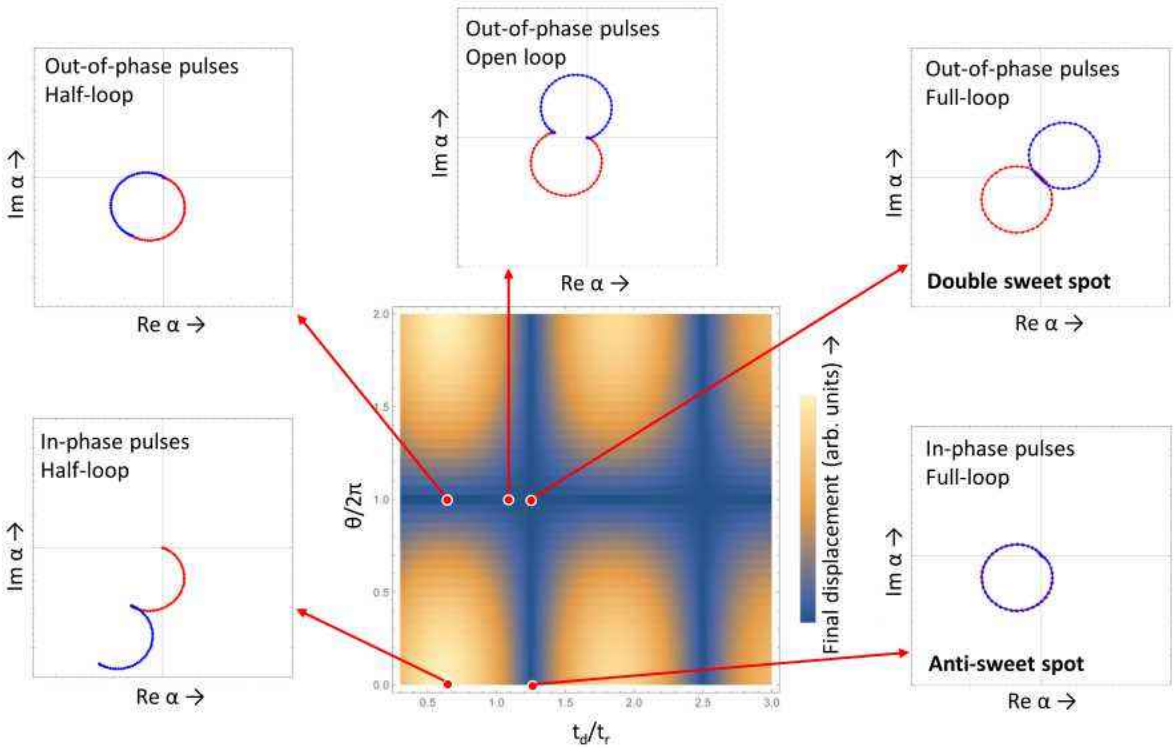

- Pulse shaping
- Smooth rectangular (SR) is optimial
- Robust in duration
- Low excitation of other (spectator) modes

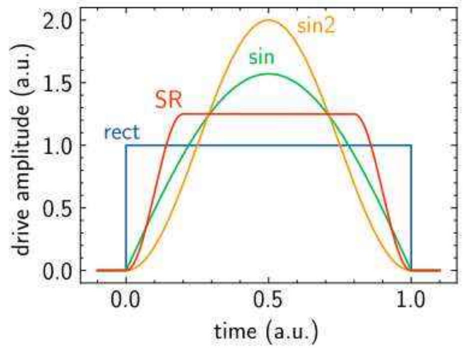

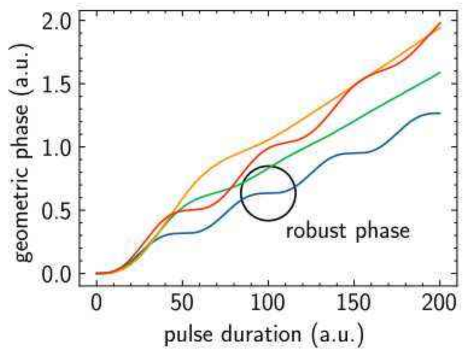

Radial 4-kick gate

- ❑ Chose 49p for better lifetime
- ❑ Spin-echo like

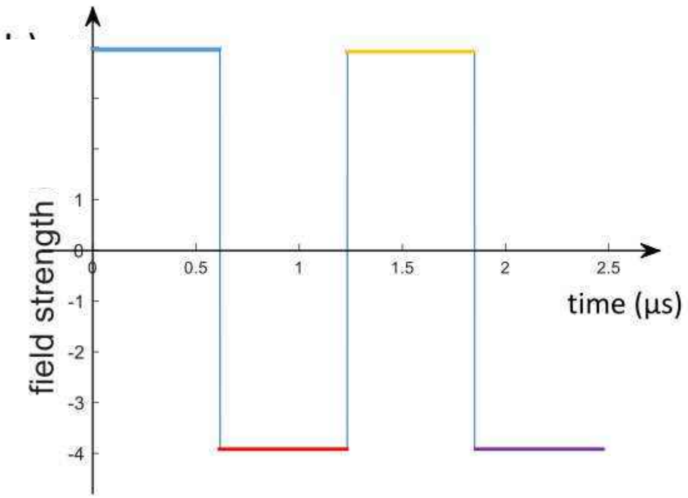

To do:

- ❑ Robustification against δV and $\delta\tau$
- ❑ all-to-all in N=10 ion crystal

Phase space trajectories:

Rock. mode

COM mode

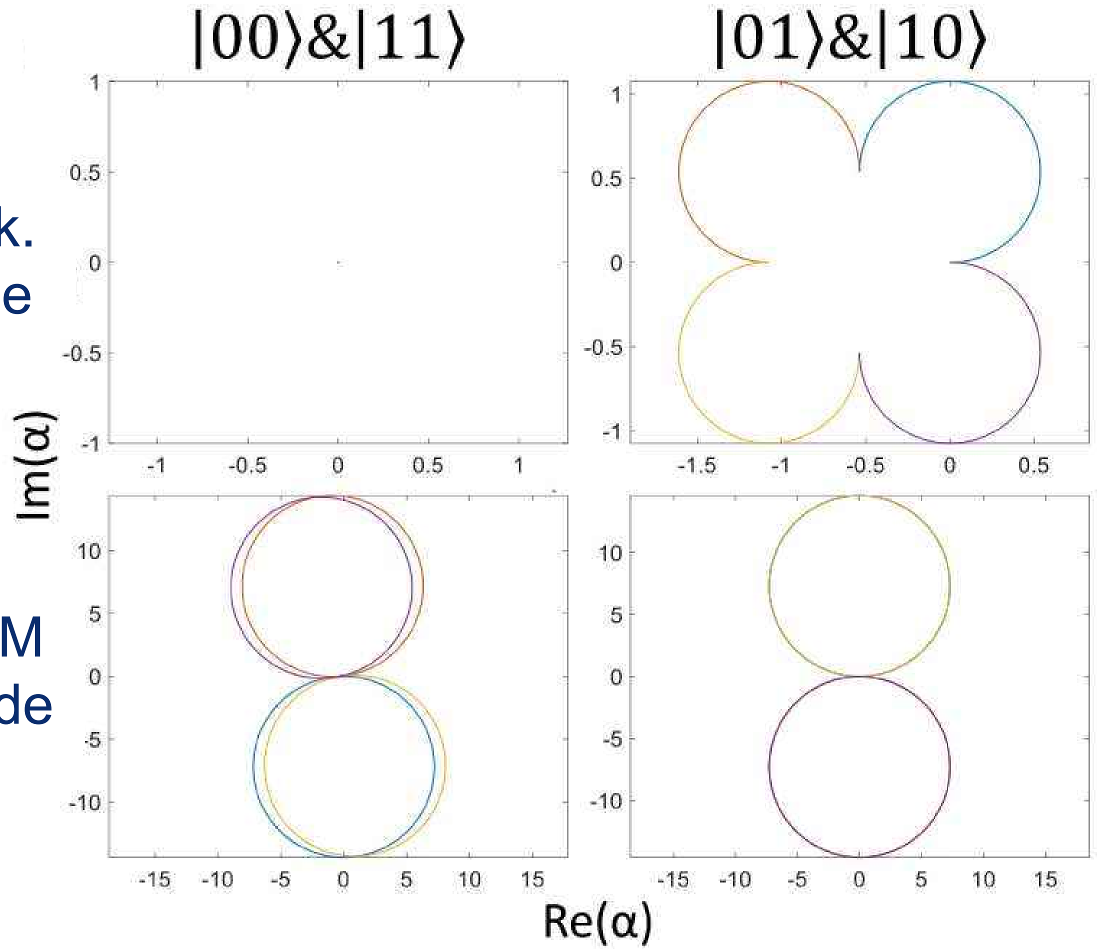

Shapira, et al. PRL 130, 030602 (2023)

H. Bao, et al. (2023)

Characterize the gate

- Cycle benchmarking is able to sense
- small gate imperfection in the presence of SPAM (state preparation and readout errors)

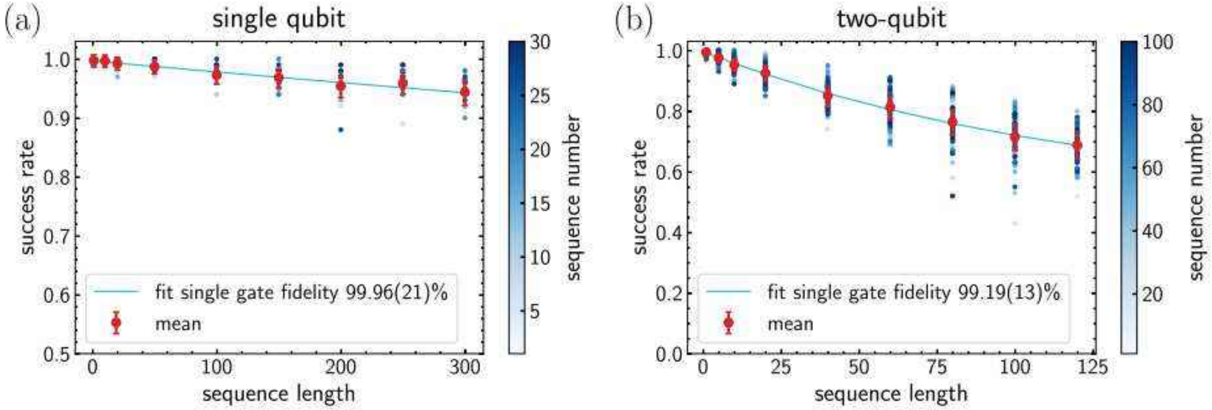

- Long term stability, here 20 gate sequence

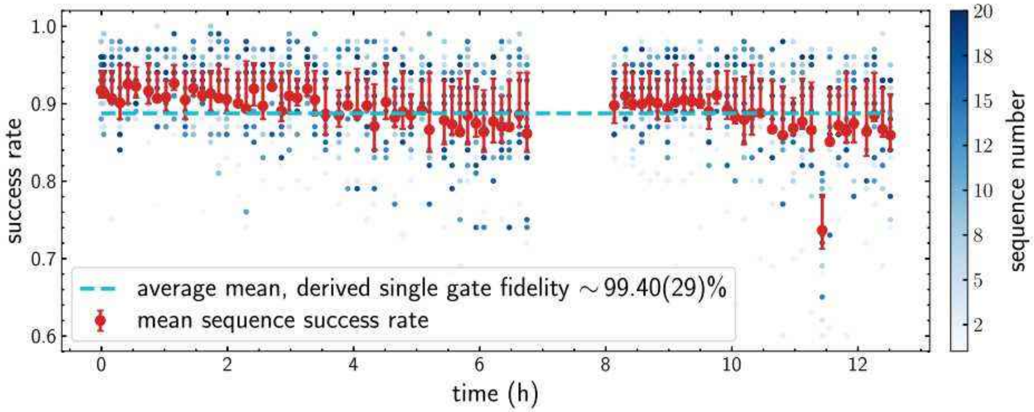

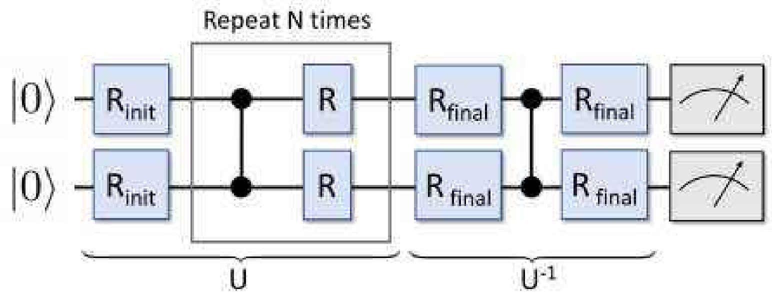

- Fighting 13T ramps from the basement with 2-layer µ-shield and active comp.
- Permanent magnet quant. B field thermal drift
- < 80Hz qubit stab

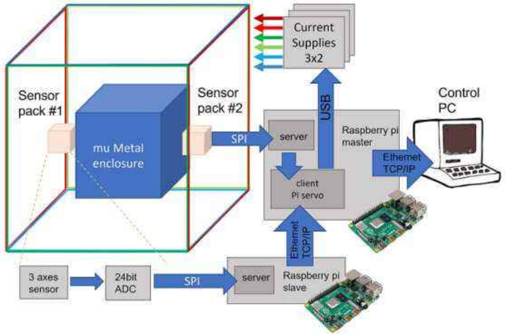

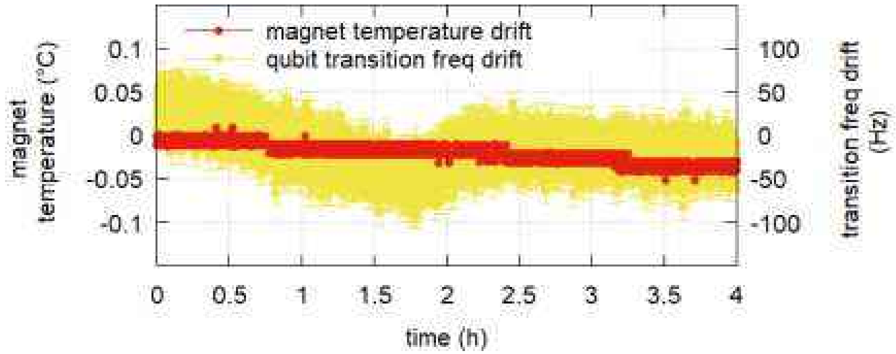

Finding a compromise:

Architecture with **different levels connectivity** of processor nodes, here color center qubits:

Number of qubits & connectivity	⟵ architecture ⟶	Controllability & crosstalk & dephasing

- ❑ Spin-spin and cavity-mediated spin interactions
- ❑ Cavity-cavity far-distance interactions
- ❑ Eventually single implanted color centers

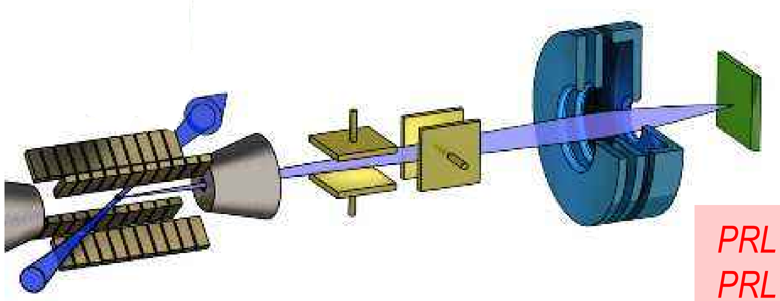

PRL 117, 043001
PRL 123, 106802

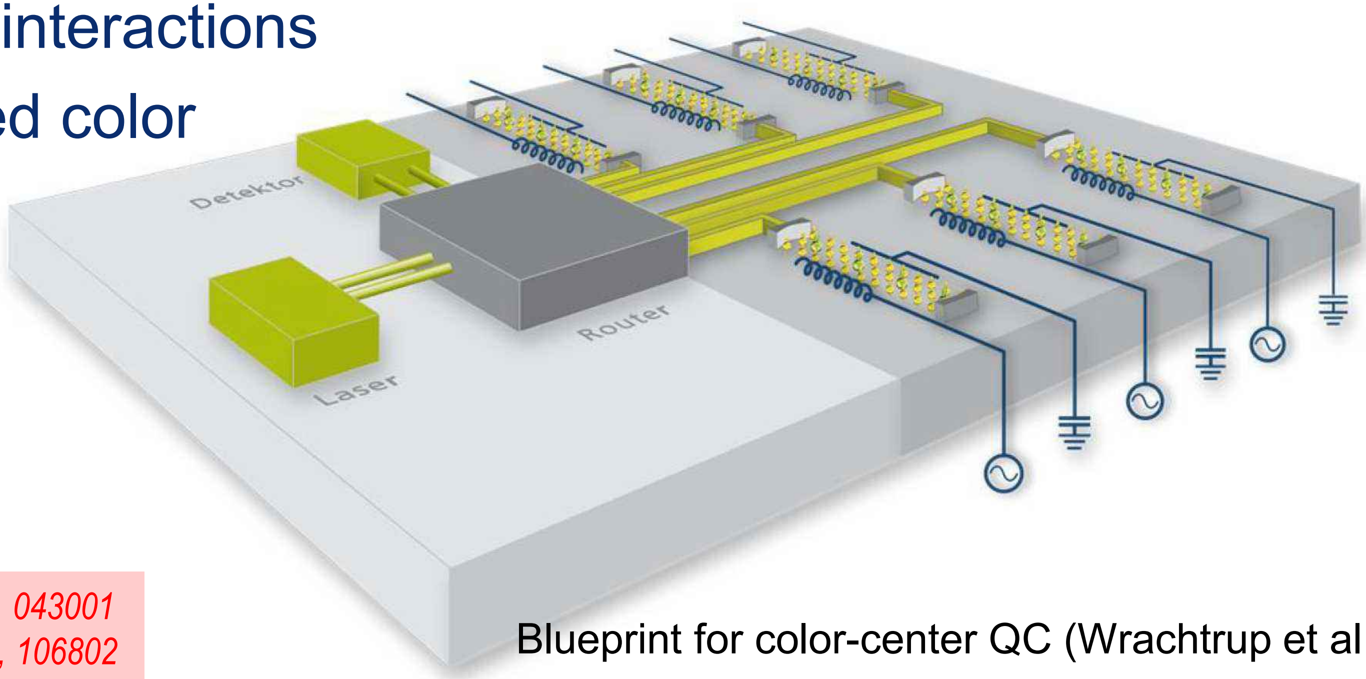

Blueprint for color-center QC (Wrachtrup et al.)

Addressability and scaling

Each qubit needs several control wires, down to the cryostate @ 20mK

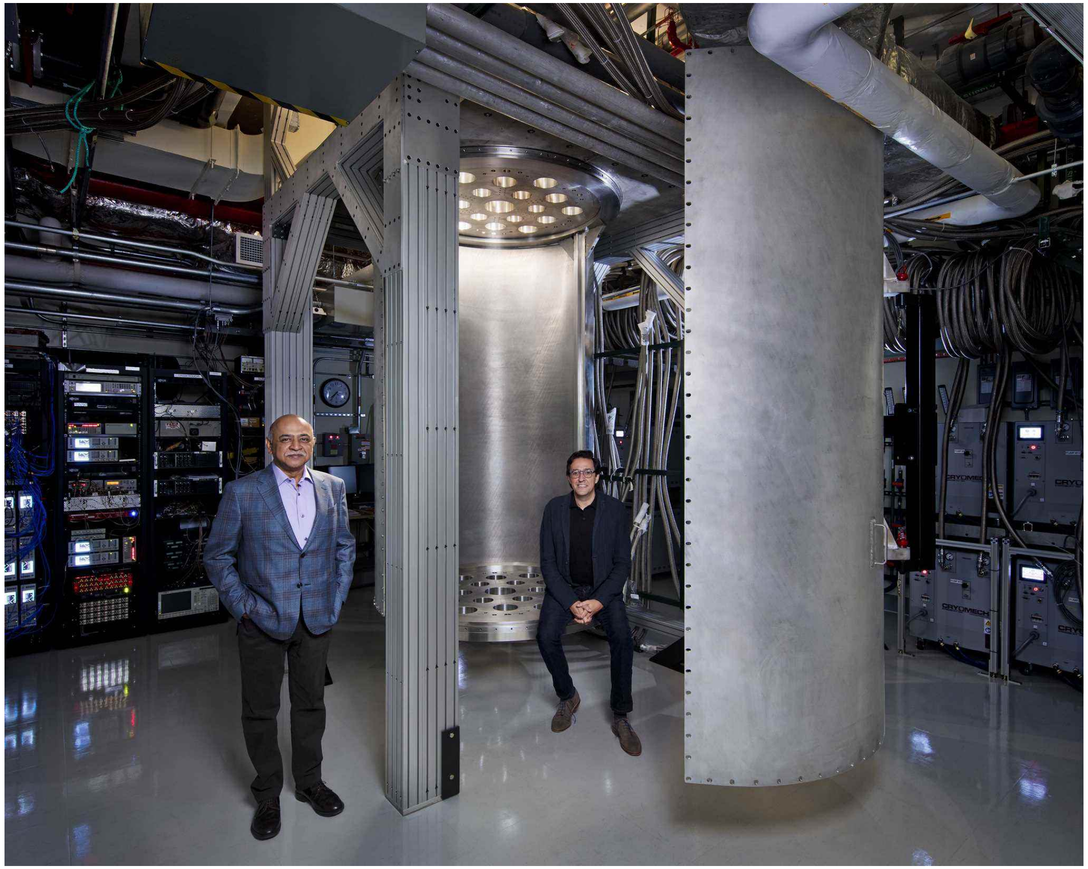

Various platforms for quantum computers

Trapped ion qubits: highest fidelities for gates and qubit preparation, longest coherence

Superconduction circuits: highest speed in gates and qubit detection

Neutral atoms: highest number of qubits

Photonic devices: fast, interconnectivity of nodes

Quantum dots, single donors: connecting to solid state processor fab. technology

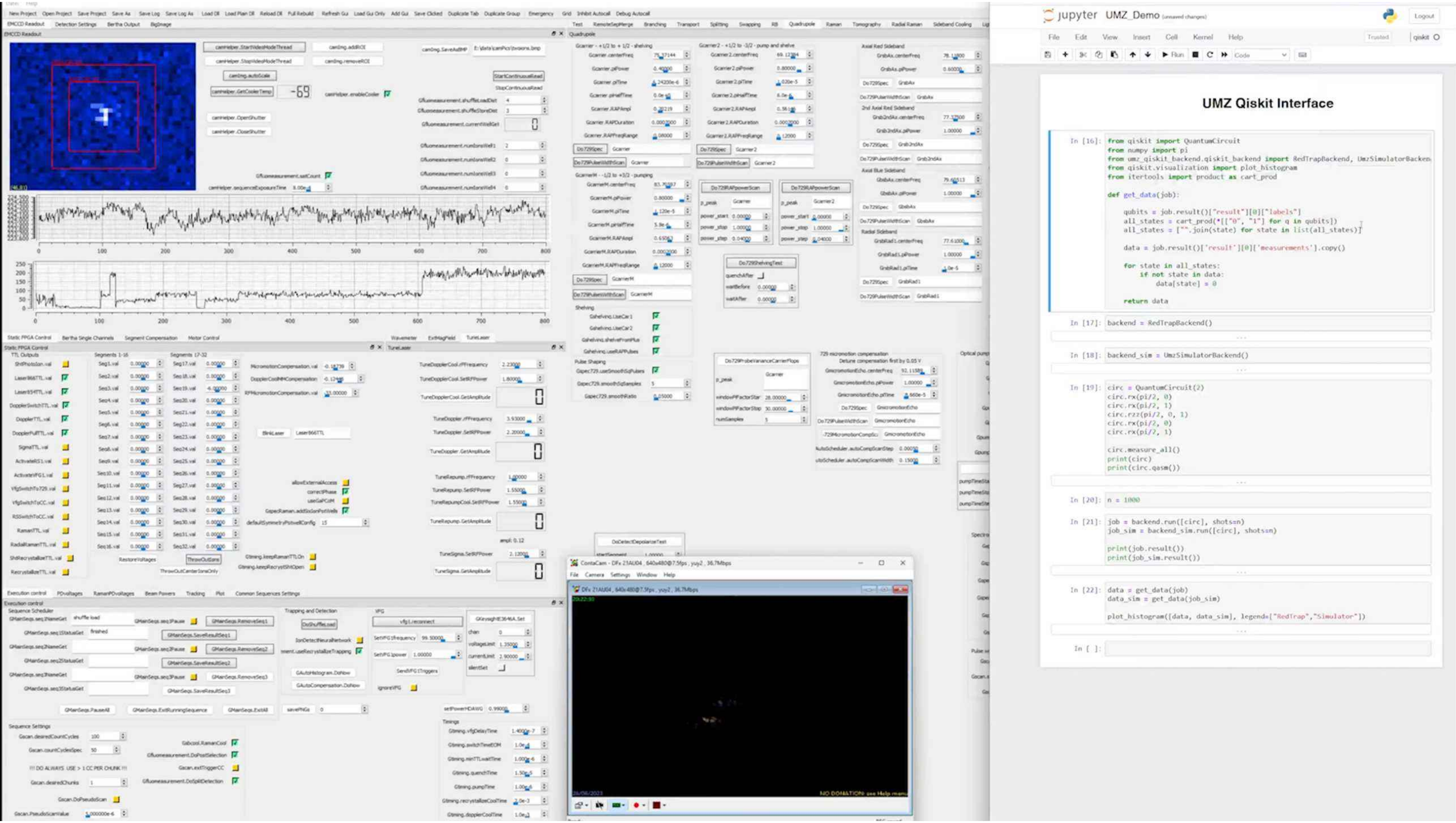
jupyter UMZ_Demo
UMZ Qiskit Interface
In [16]:
from qiskit import QuantumCircuit
from numpy import pi
from umz_qiskit_backend.qiskit_backend import RedTrapBackend, UmzSimulatorBacken
from qiskit.visualization import plot_histogram
from itertools import product as cart_prod
def get_data(job):
qubits = job.result()["result"][0]["labels"]
all_states = cart_prod(*[["0", "1"] for q in qubits])
all_states = ["".join(state) for state in list(all_states)]
data = job.result()['result'][0]['measurements'].copy()
for state in all_states:
if not state in data:
data[state] = 0
return data
In [17]: backend = RedTrapBackend()
In [18]: backend_sim = UmzSimulatorBackend()
In [19]:
circ = QuantumCircuit(2)
circ.rx(pi/2, 0)
circ.rx(pi/2, 1)
circ.rzz(pi/2, 0, 1)
circ.rx(pi/2, 0)
circ.rx(pi/2, 1)
circ.measure_all()
print(circ)
print(circ.qasm())
In [20]: n = 1000
In [21]:
job = backend.run([circ], shots=n)
job_sim = backend_sim.run([circ], shots=n)
print(job.result())
print(job_sim.result())
In [22]:
data = get_data(job)
data_sim = get_data(job_sim)
plot_histogram([data, data_sim], legend=["RedTrap","Simulator"])
In [ ]:

Linear crystal processor

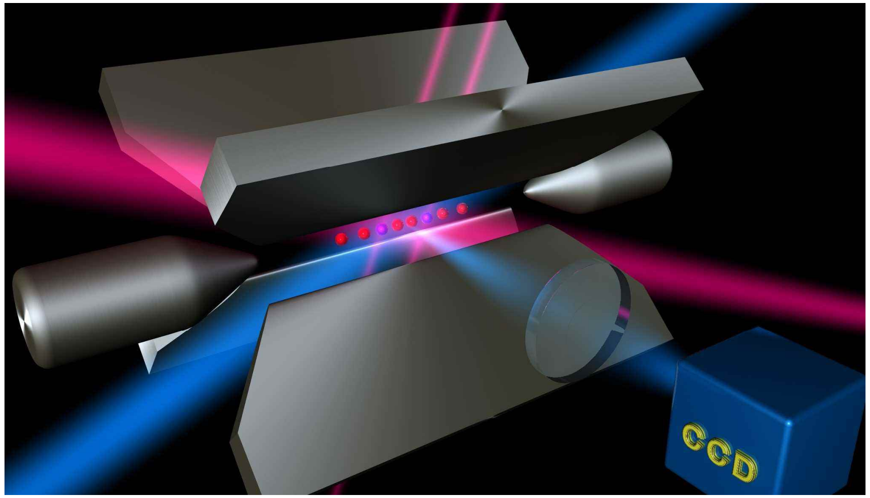

- Static trapped ion registers >20 qubits
- Individual single ion addressing for gates

Nägerl, et al, PRA 60, 145 (1999)
Friis, et al, Phys Rev X. 8 021012 (2018)
Korenblit et al, NJP 14, 095024 (2012)
Egan et al., Nat. 598, 281 (2021)

Quantum-CCD architecture

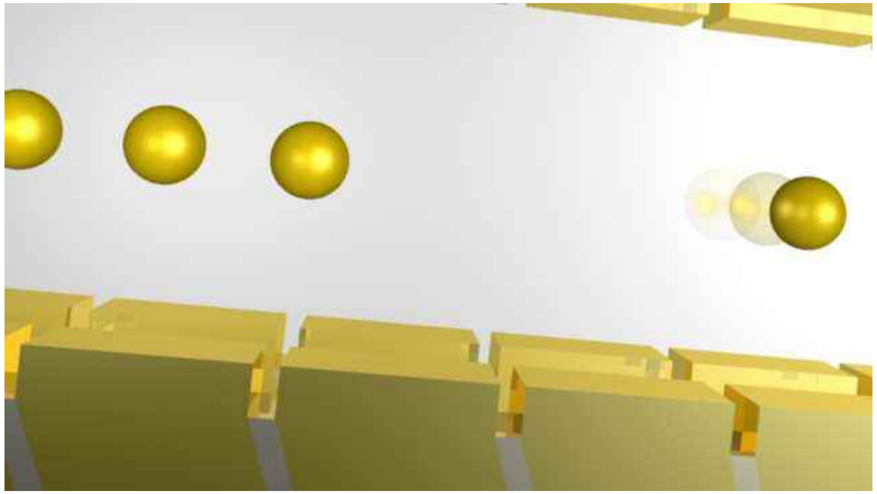

- Segmented micro trap allows for controlling the ion positions

Kielpinski et al., Nat. 417, 709 (2002)
Kaustal et al, Adv. At. Mol. Opt. Phys. 69, 233 (2020)
Ryan-A. et al, Phys. Rev. X 11, 041058 (2021)
Hilder et al., Phys. Rev. X 12, 011032 (2022)

Multi-Flavor Schwinger Model VQE

We adopt a lattice formulation with Kogut-Susskind staggered fermions [36]. In the temporal gauge, and in absence of a background field, the Hamiltonian for F flavors on a lattice with spacing a and N sites reads

$$
\begin{aligned}
H = &-\frac{i}{2a}\sum_{n=0}^{N-2}\sum_{f=0}^{F-1}(\phi_{n,f}^{\dagger}e^{i\theta_n}\phi_{n+1,f} - \mathrm{H.c.}) \\
&+\sum_{n=0}^{N-1}\sum_{f=0}^{F-1}[m_f(-1)^n + \kappa_f]\phi_{n,f}^{\dagger}\phi_{n,f} \\
&+\frac{ag^2}{2}\sum_{n=0}^{N-2}L_n^2. \qquad (1)
\end{aligned}
$$

Banuls, et al, PRL 118, 071601 (2017)

- ❑ High-energy Hamiltonian H
- ❑ Minimal model: three flavours and two Fermions

- ❑ Wigner transformation in circuit

$$
\begin{aligned}
W = &\,2\sqrt{x}\left(\frac{\kappa_0}{g}+\frac{\kappa_1}{g}+\frac{\kappa_2}{g}+\frac{3}{2\sqrt{x}}\right)\mathbb{1} + \sqrt{x}\left(\frac{m_0}{g}+\frac{\kappa_0}{g}+\frac{3}{2\sqrt{x}}\right)\sigma_0^z \\
&+\sqrt{x}\left(\frac{m_1}{g}+\frac{\kappa_1}{g}+\frac{3}{2\sqrt{x}}\right)\sigma_1^z + \sqrt{x}\left(\frac{m_2}{g}+\frac{\kappa_2}{g}+\frac{3}{2\sqrt{x}}\right)\sigma_2^z \\
&+\sqrt{x}\left(\frac{\kappa_0}{g}-\frac{m_0}{g}\right)\sigma_3^z + \sqrt{x}\left(\frac{\kappa_1}{g}-\frac{m_1}{g}\right)\sigma_4^z + \sqrt{x}\left(\frac{\kappa_2}{g}-\frac{m_2}{g}\right)\sigma_5^z \\
&+\frac{1}{2}\sigma_0^z\sigma_1^z + \frac{1}{2}\sigma_0^z\sigma_2^z + \frac{1}{2}\sigma_1^z\sigma_2^z + \frac{x}{2}\sigma_0^x\sigma_1^z\sigma_2^z\sigma_3^x + \frac{x}{2}\sigma_0^y\sigma_1^z\sigma_2^z\sigma_3^y \\
&+\frac{x}{2}\sigma_1^x\sigma_2^z\sigma_3^z\sigma_4^x + \frac{x}{2}\sigma_1^y\sigma_2^z\sigma_3^z\sigma_4^y + \frac{x}{2}\sigma_2^x\sigma_3^z\sigma_4^z\sigma_5^x + \frac{x}{2}\sigma_2^y\sigma_3^z\sigma_4^z\sigma_5^y\,.
\end{aligned}
$$

- ❑ Quantum processor delivers <W> dep. on chem. potential & masses
- ❑ Classical minimum search
- ❑ Learn about flavour phases and transitions

Multi-Flavor Schwinger circuit for W

- Enter openquasim as pyton code for 6 qubits
- Optimize quantum circuit
- Convert into our native gate set
- Generate shuttling sequence

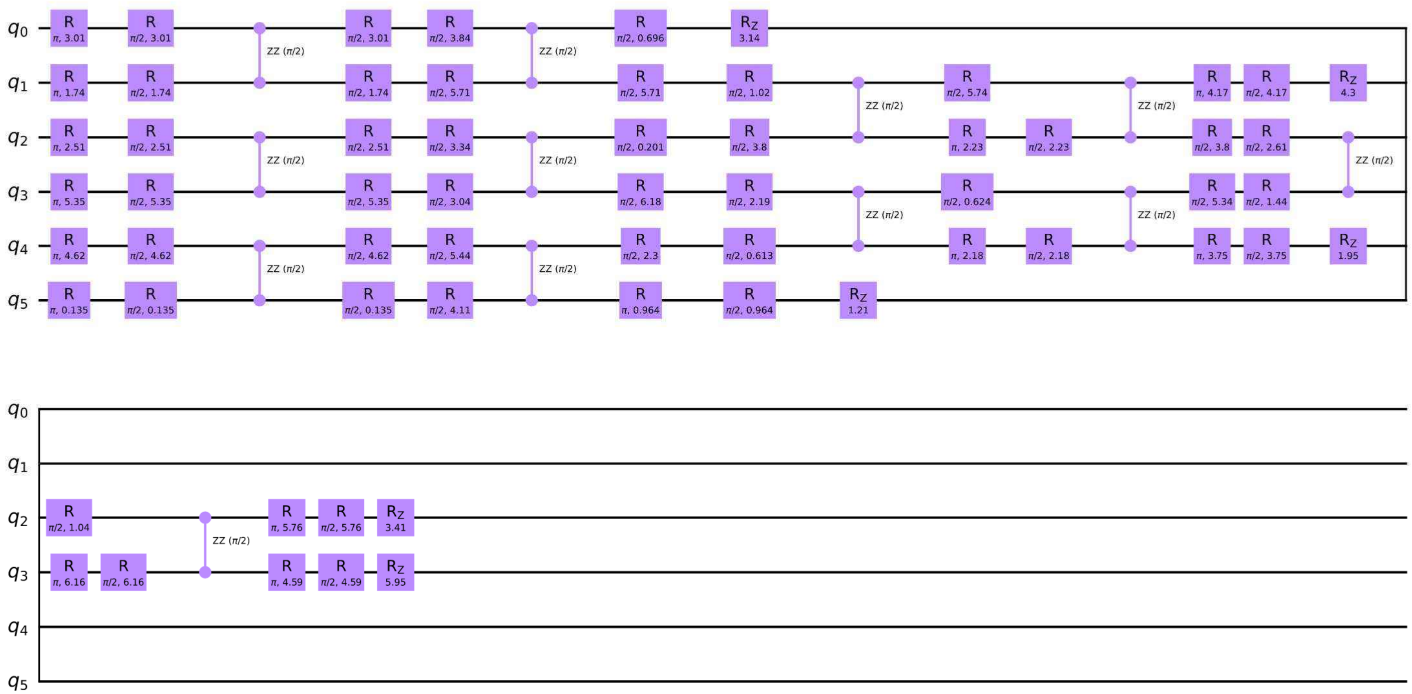

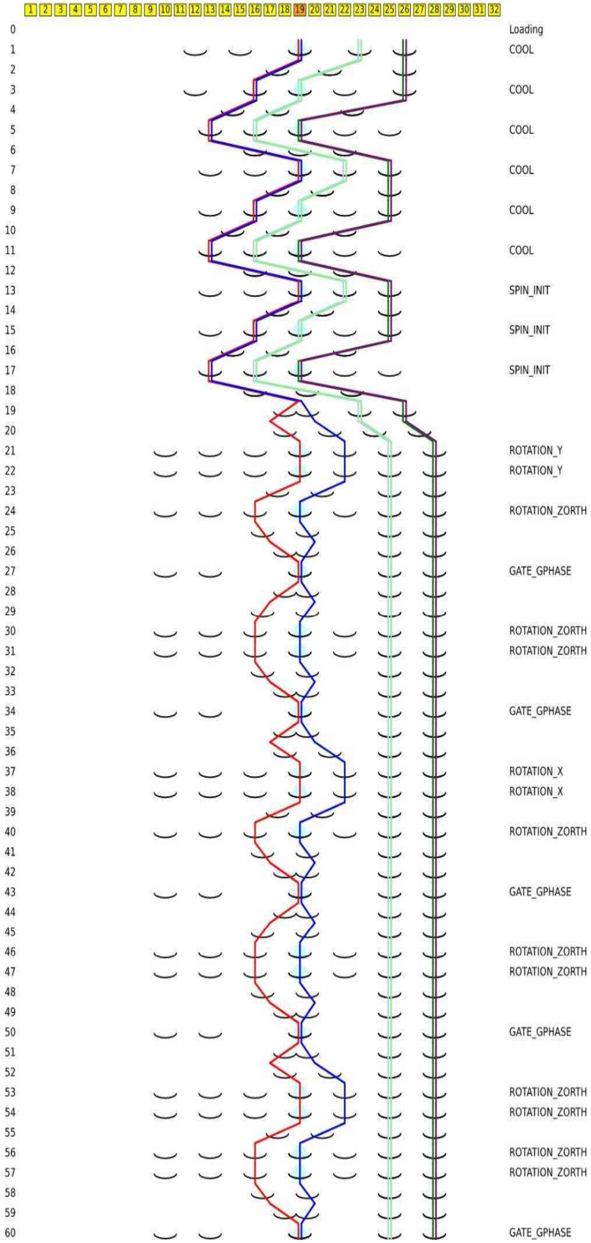

Rydberg energies and quantum defect

- $nS_{1/2}$ states $38 \le n \le 65$
- $nD_{5/2}$ states $37 \le n \le 50$
- Ionization energy I^{++}=2 870 575.582(15) GHz
- Quantum defects:

  μ^S =1.802995(5) μ^D =0.626888(9)

x60

Rydberg Ritz formula

$$E_{n,l,j} = I^{++} - \frac{Z^2 R^*}{(n-\mu(E))^2} + \frac{Z^4 \alpha^2 R^*}{(n-\mu(E))^3}\left[\frac{3}{4(n-\mu(E))} - \frac{1}{(j+1/2)}\right]$$

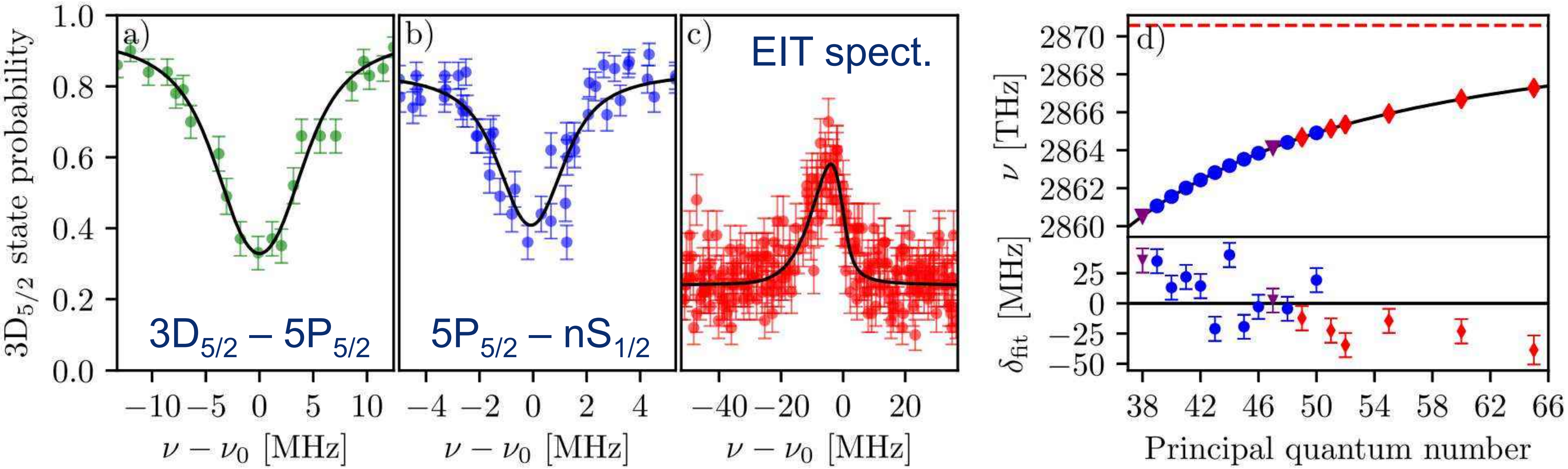

Rydberg-induced depopulation rate

- ❑ Rate up determined by matrix dipole moment ~ $n^{-3/2}$
- ❑ Rate down determined by Rydberg life time
- ❑ Resulting depopulation rate ~ $n^{-3.0(0.4)}$
- ❑ Agreement with expected n-scaling

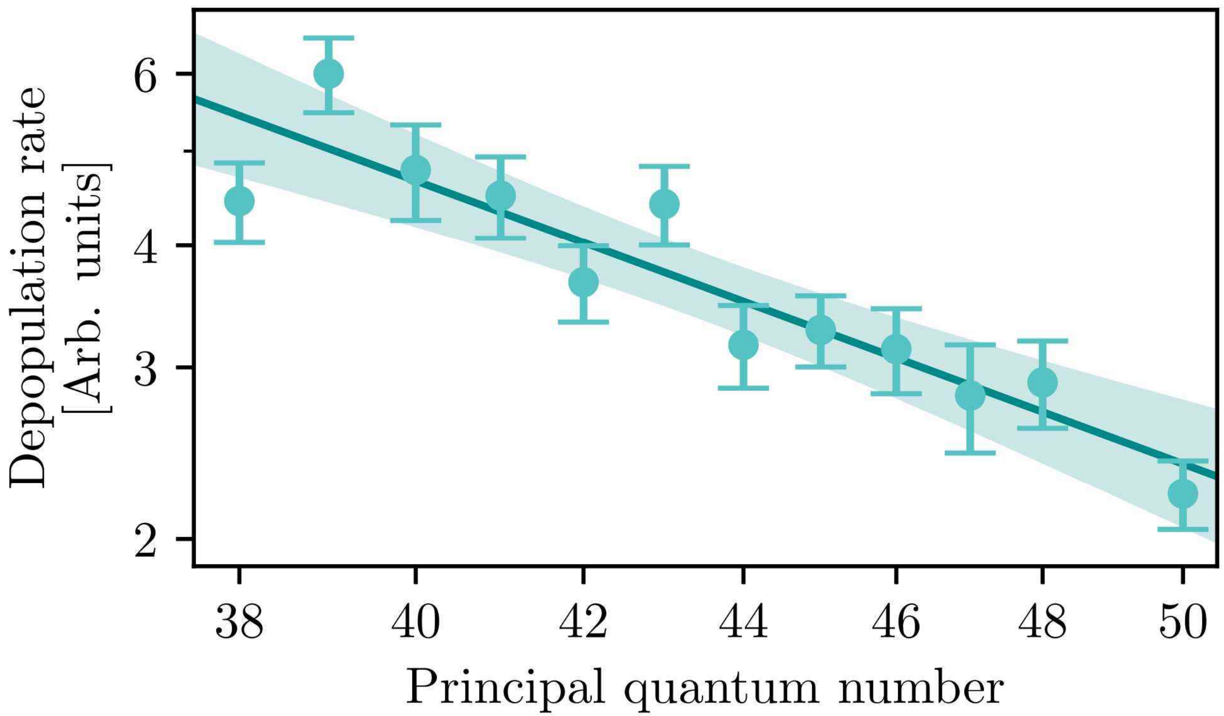

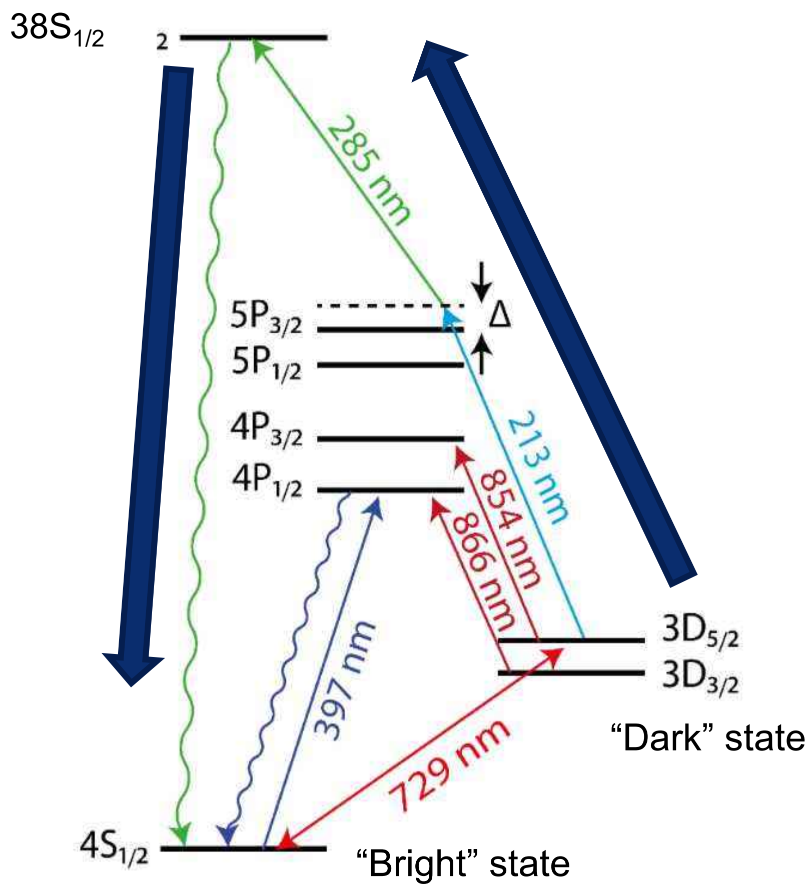

Andrijauskas et al., PRL 127, 203001 (2021)

Adv. At. Mol. Opt. Phys. 69, 233 arXiv:2009.01070

Rydberg ion stability in the trap

- Loss rates of 1.8... 8 x 10^{-3}
- Double-ionization dominates „loss“ rate

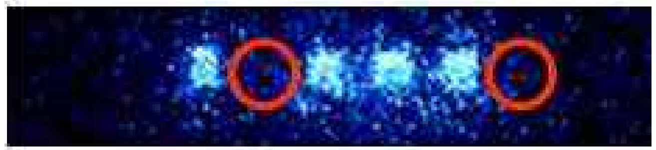

- Scaling ~ $n^{-5.7(0.9)}$
- Blackbody radiation induced transitions scaling ~ n^{-5}
- Cryo setup investigated

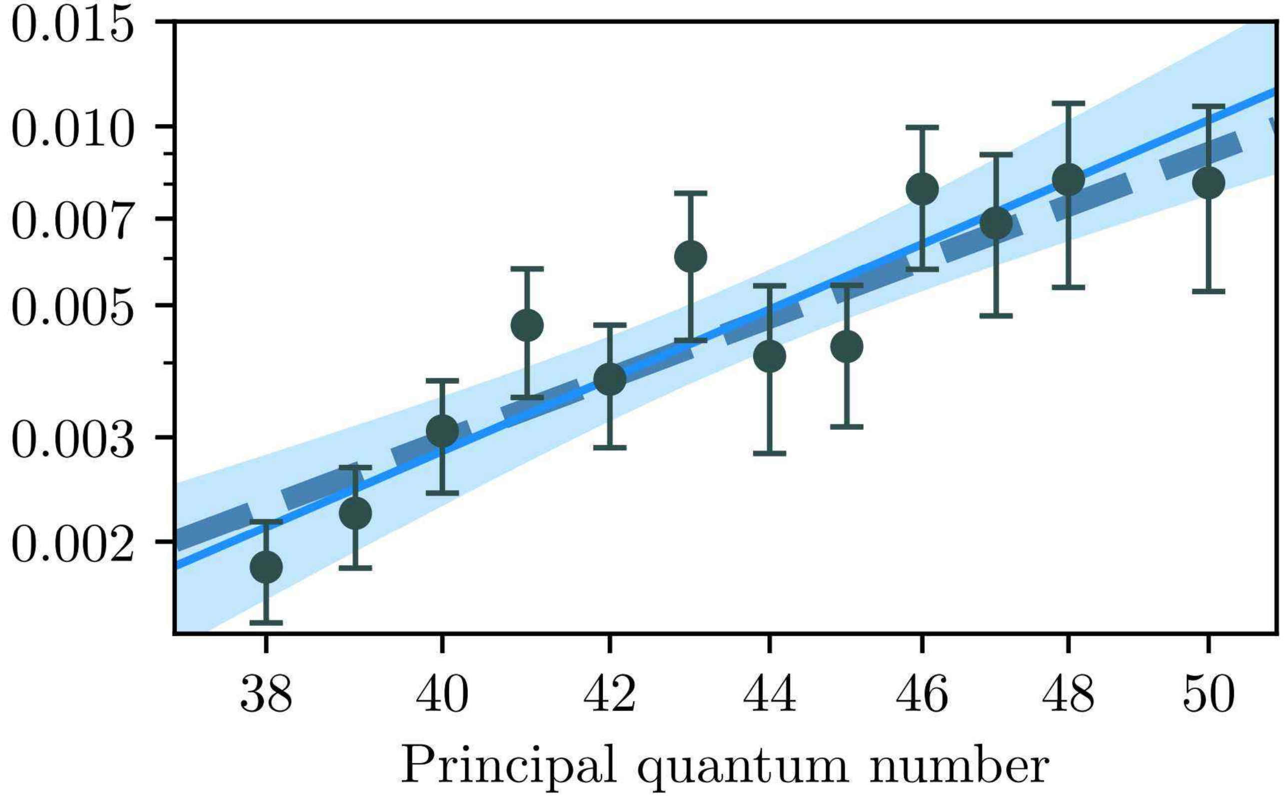

Beterov, et al., PRA 79, 052504 (2009)

Vogel et al, PRL123, 153603 (2019)

Kicking ion crystal for entanglement

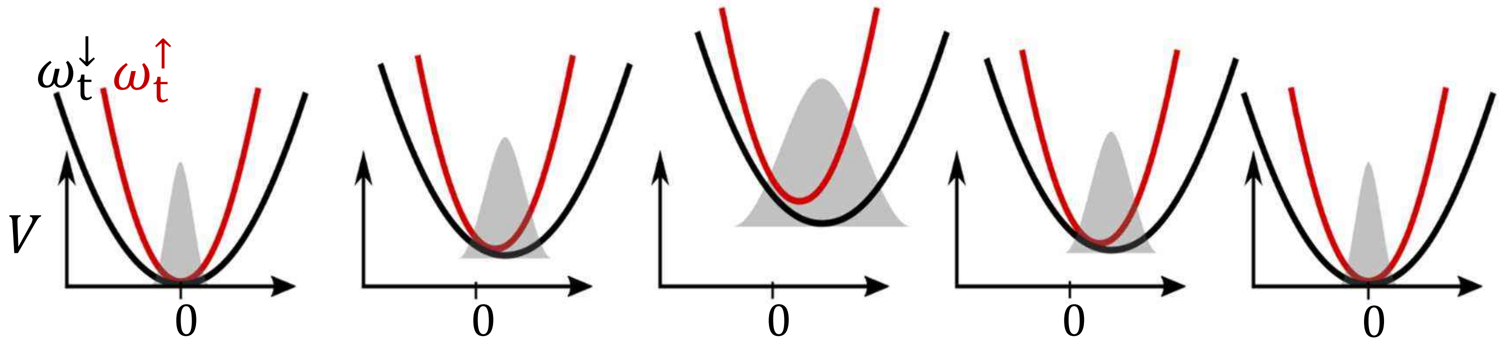

- Kick two-ion crystal
- Optimize kick strenght f(t), kick duration τ
- Generate a difference of phase π for ↓, and ↑
- Phase gate operation within sub-μs possible

$$U_{\mathrm{CP}} = \begin{pmatrix} 1 & 0 & 0 & 0 \\ 0 & 1 & 0 & 0 \\ 0 & 0 & 1 & 0 \\ 0 & 0 & 0 & -1 \end{pmatrix}$$

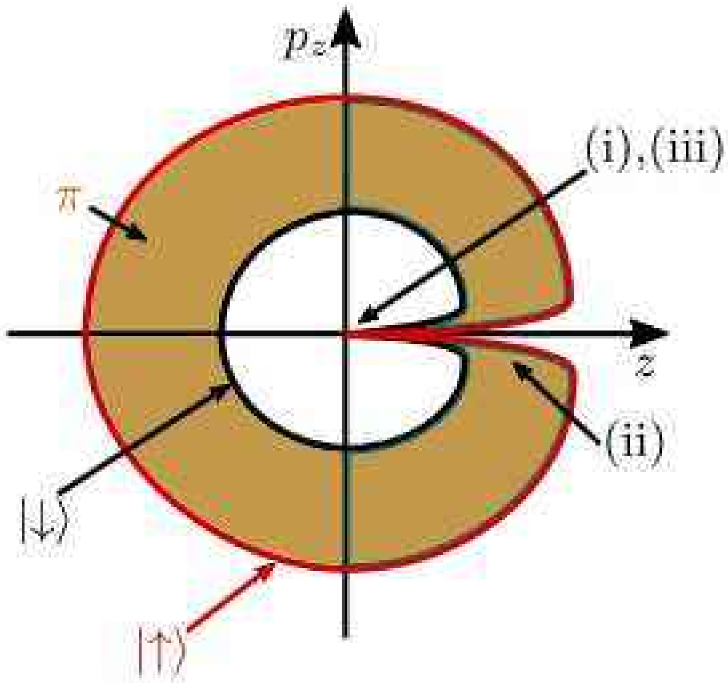

H. Bao, et al. (2023)

Radial continuous displacement gate

- ❑ Smooth voltage waveform

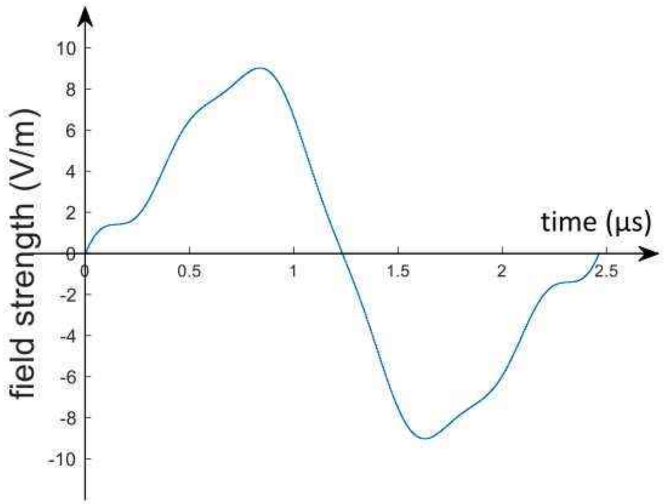

Phase space trajectories:

Rock. mode

COM mode

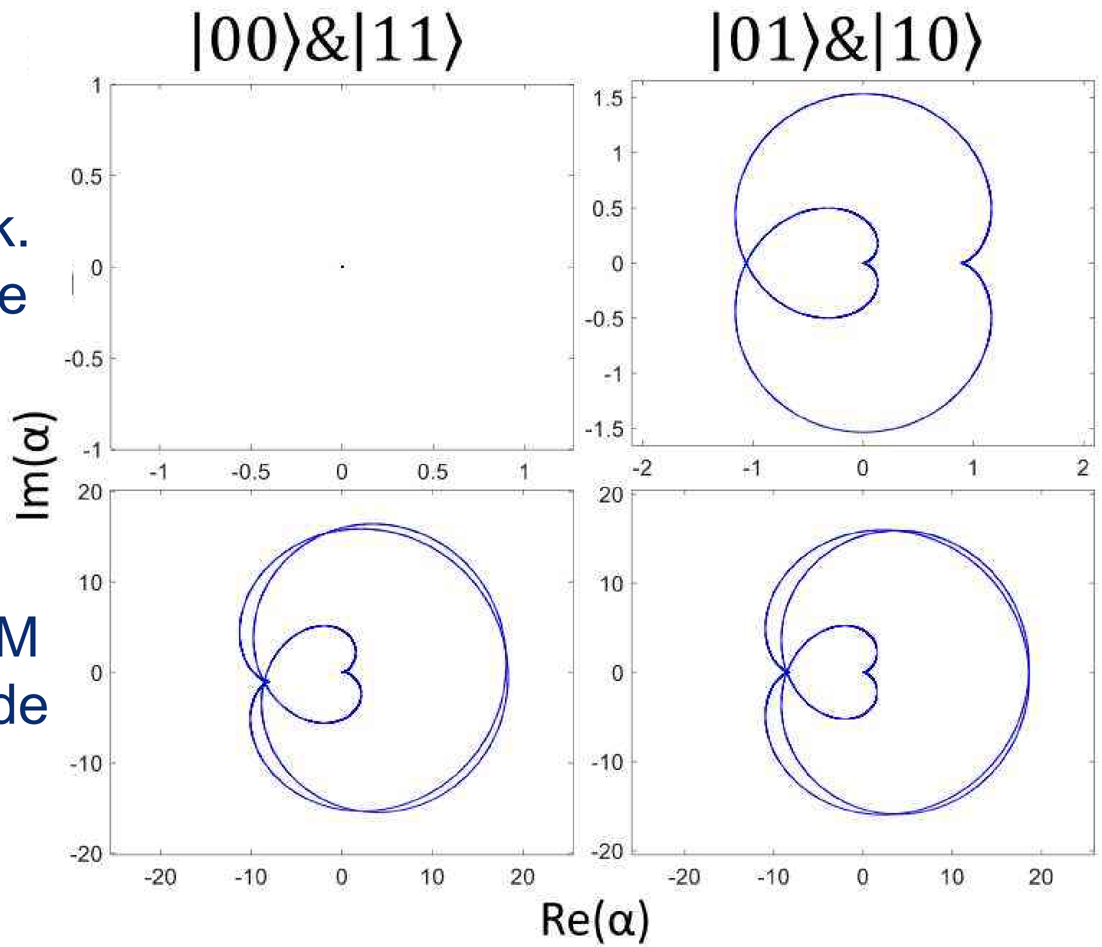

Radial multi-kick gate

H. Bao, et al. (2023)

- Chose 49p for better lifetime, fidelity limited by lifetime
- Kick sequence 10 .. 100ns
- „hot“ gate, motional state infidelity ~ 10^{-4}

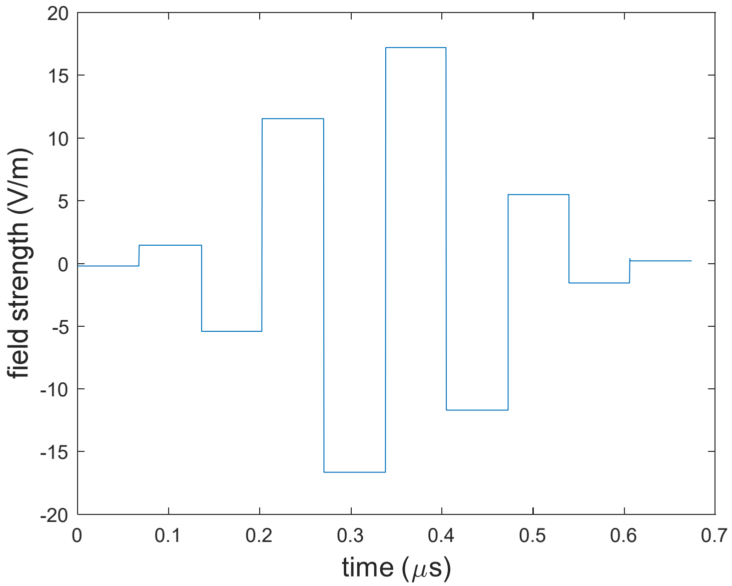

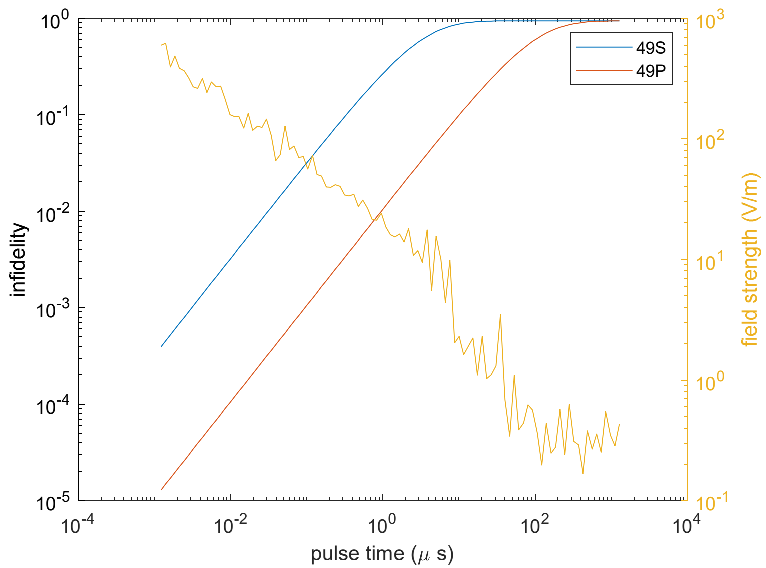

Phase space trajectories:

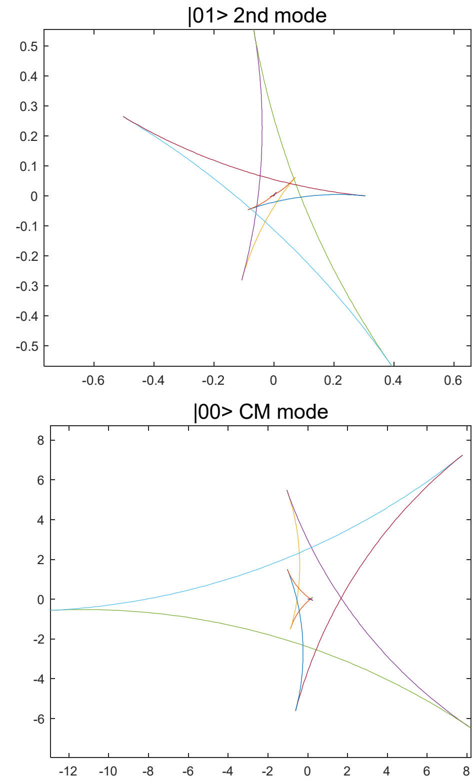

To do:

- Robustification against δV and $\delta\tau$
- all-to-all in N=10 ion crystal

Shapira, et al. PRL 130, 030602 (2023)

Niederländer et al, arXiv:2208.11117, NJP (2023)

Polarizability measurement

- Calibrate the coherent state by sideband spectroscopy
- Fit the line shift
- Determine polarizability for different states nS (in future nD, nP)